https://doi.org/10.5194/npg-2022-15
Preprint. Discussion started: 19 October 2022

Nonlinear Processes in Geophysics
Discussions
Open Access
EGU

The Role of Internal Variability in Regional Climate Change

Clara Deser* and Adam S. Phillips

National Center for Atmospheric Research, Boulder CO USA

EGU Nonlinear Processes in Geophysics Special Issue

"Interdisciplinary perspectives on climate sciences – highlighting past and current scientific achievements"

* Corresponding author: Clara Deser cdeser@ucar.edu

https://doi.org/10.5194/npg-2022-15
Preprint. Discussion started: 19 October 2022

Nonlinear Processes in Geophysics
Discussions
Open Access
EGU

15 **Abstract**

16 Disentangling the effects of internal variability and anthropogenic forcing on regional climate
17 change remains a key challenge with far-reaching implications. Due to its largely unpredictable
18 nature on timescales longer than a decade, internal climate variability limits the accuracy of climate
19 model projections, introduces challenges in attributing past climate changes, and complicates
20 climate model evaluation. Here, we highlight recent advances in climate modeling and physical
21 understanding that have led to novel insights on these key issues. In particular, we synthesize new
22 findings from Large Ensemble simulations with Earth System Models, Observational Large
23 Ensembles, and "dynamical adjustment" methodologies, with a focus on European climate.

24

25 **1. Introduction**

26 ***a. Internal variability and forced climate change***

27 The climate system is highly variable in both space and time. This variability originates from
28 processes within the coupled ocean-atmosphere-cryosphere-land-biosphere system, as well as
29 from external influences such as solar and orbital cycles, volcanic eruptions, and anthropogenic
30 emissions of greenhouse gases and sulfate aerosols. A primary source of internally-generated
31 variability is the atmospheric general circulation, which produces familiar day-to-day and week-
32 to-week weather fluctuations. The non-linear nature of atmospheric dynamics limits predictability
33 to less than a few weeks; beyond this time scale, atmospheric motions may be considered as
34 random stochastic processes, often termed "weather noise" (e.g., Lorenz, 1963; Leith, 1973; James
35 and James, 1992). It is important to note that such "weather noise" imparts variability on a
36 continuum of time scales, from sub-monthly to decadal and longer (e.g., Madden, 1975; Deser et
37 al. 2012; Thompson et al. 2015).

https://doi.org/10.5194/npg-2022-15
Preprint. Discussion started: 19 October 2022


Nonlinear Processes in Geophysics
Discussions
Open Access
EGU

38

39 Another important source of internally-generated variability is the coupling between the ocean and
40 atmosphere. Large-scale air-sea interactions give rise to distinctive patterns (or "modes") of
41 variability on interannual and longer time scales, including phenomena such as "El Niño –
42 Southern Oscillation" (ENSO; Wang et al. 2017), "Pacific Decadal Variability" (PDV; Newman
43 et al. 2016) and "Atlantic Multi-decadal Variability" (AMV; Zhang et al. 2019). Like the
44 atmospheric general circulation, these coupled modes are governed by non-linear dynamical
45 processes which limit their predictability. For example, forecast skill is generally limited to 1-2
46 years for ENSO (Jin et al., 2008; DiNezio et al. 2017; Wu et al. 2021), 5 years for PDV (Teng and
47 Branstator, 2010; Meehl et al., 2016; Gordon and Barnes, 2022) and 10 years for AMV (Griffies
48 and Bryan, 1997; Trenary and DelSole, 2016; Yeager et al., 2020). Beyond these predictability
49 time horizons, internally-generated variability can be thought of as a "roll of the dice", introducing
50 unavoidable uncertainty to climate model projections especially at local and regional scales (e.g.,
51 Deser et al. 2012, 2014 and 2020).

52

53 Not only does unpredictable internal variability cause irreducible uncertainty in future climate
54 projections, it also confounds interpretation of the historical climate record. For example, internal
55 variability may partially obscure the regional climate response to external forcings including
56 industrial greenhouse gas emissions, stratospheric ozone depletion and volcanic eruptions
57 (Wallace et al., 2013; Schneider et al. 2015; Lehner et al. 2016; McGraw et al. 2016). In some
58 areas, climate trends driven by internal processes may even outweigh those due to anthropogenic
59 influences over the past 30-60 years (Deser et al., 2012, 2016 and 2017; Wallace et al., 2013; Swart
60 et al. 2015; Lehner et al. 2017). The co-existence of internal and anthropogenic influences

https://doi.org/10.5194/npg-2022-15
Preprint. Discussion started: 19 October 2022


Nonlinear Processes in Geophysics Discussions

necessitates a probabilistic approach to detection and attribution of the human contribution to anomalous weather and climate events.

The prevalence of internal climate variability also complicates model evaluation efforts, since the simulated temporal sequence of (unpredictable) internal variability need not match observations even if the model's physics are realistic. Further, the brevity of the instrumental record provides only a limited sampling of internal variability, hindering robust model evaluation. Thus, climate models may show an apparent bias with respect to observations, but this could be entirely attributable to sampling issues rather than indicative of a true bias due to incorrect model physics. Apparent model bias due to sampling uncertainty must be kept in mind when assessing fidelity of simulated modes of internal variability (e.g., Wittenberg et al. 20xx; Deser et al. 2017; Capotondi et al. 2020; Fasullo et al. 2021; McKenna and Maycock, 2021), transient climate sensitivity (Dong et al. 2021; Andrews et al. 2022), and "signal-to-noise" properties of initial-value predictions and forced responses (e.g., Scaife and Smith, 2018; Smith et al., 2020; Klavans et al. 2021). In particular, even with 100 years of data, sampling uncertainty is a limiting factor for evaluating ENSO properties in climate models, including its global atmospheric teleconnections and associated climate impacts (Deser et al. 2017 and 2018; Capotondi et al. 2020) and forced changes thereof (Stevenson et al. 2012; Maher et al. 2018; Maher et al. 2022; O'Brien and Deser, 2022). This issue is particularly acute for model assessment of modes of decadal variability such as PDV and AMV due to the paucity of samples in the short instrumental record (Deser and Phillips 2021; Fasullo et al. 2021).

b. Initial-condition Large Ensemble Simulations with Earth System Models

https://doi.org/10.5194/npg-2022-15
Preprint. Discussion started: 19 October 2022


Nonlinear Processes in Geophysics Discussions

To overcome the issue of sampling uncertainty, a recent thrust in climate modeling is to run a large number of simulations (30-100) with the same coupled model and the same radiative forcing protocol (historical and/or future scenario) but vary the initial conditions. The initial-condition variation can be accomplished by introducing a random perturbation to the atmosphere on the order of the model's numerical round-off error (e.g., 10^{-14} K in the case of atmospheric temperatures; Kay et al. 2015) or it can be done by selecting a different ocean state from a long control run of the coupled model, or a combination of the two (Deser et al. 2020 and Rodgers et al. 2021). Regardless of the method used, the initial-condition perturbation serves to create ensemble spread once the memory of the initial state is lost, typically within a month for the atmosphere and a few years to a couple of decades for the ocean. The ensuing ensemble spread is thus solely attributable to random internal variability (e.g., the "butterfly effect" in chaos theory); see Lorenz (1963) and Tel et al. (2019). Because the temporal sequences of internal variability unfold differently in the various ensemble members once the memory of the initial conditions is lost, one can estimate the forced component at each time step (at each location) by averaging the members together, provided the ensemble size is sufficiently large. The internal component in each ensemble member is then obtained as a residual from the ensemble-mean. Note that a larger ensemble may be needed for some aspects of the forced response than others: for example, forced changes in ocean heat content may be readily detected with just a few members, while forced changes in the characteristics of internal variability may require a much larger ensemble (Milinski et al., 2020).

Initial-condition Large Ensembles (LEs for short) have proven enormously useful for separating internal variability and forced climate change on regional scales in models, and for providing robust sampling of models' internal variability by pooling together all of the ensemble members

https://doi.org/10.5194/npg-2022-15
Preprint. Discussion started: 19 October 2022


Nonlinear Processes in Geophysics Discussions

(e.g., Deser et al., 2012; Kay et al., 2015; Maher et al., 2019; Deser et al. 2020; Lehner et al., 2020). They have also been used to assess externally-forced changes in the characteristics of simulated internal variability, including extreme events for which large sample sizes are crucial (e.g., Tebaldi et al., 2021; O'Brien and Deser, 2022). Additionally, they have served as methodological testbeds for evaluating approaches to detection and attribution of anthropogenic climate change in the (single) observational record (e.g., Deser et al., 2016; Barnes et al., 2019; Sippel et al., 2019 and 2021; Santer et al. 2019; Bonfils et al., 2019; Wills et al., 2020). Until the advent of LEs, it was problematic to identify the sources of model differences in the Coupled Model Intercomparison Project (CMIP) archives due to the limited number of simulations (generally < 3) for each model (i.e., structural uncertainty was confounded with uncertainty due to internal variability). This concern has been largely alleviated thanks to the recent availability of LEs with multiple earth system models (e.g., Deser et al. 2020; Lehner et al., 2020).

c. Observationally-based Large Ensemble

Just as in a model LE, the sequence of internal variability in the real world could have unfolded differently. That is, the observational record traces only one of many possible climate histories that could have happened under the same external radiative forcing. For example, El Niño and La Niña events could have occurred in a different set of years, and positive or negative regimes of PDV and AMV could have taken place in different decades. This concept of alternate chronologies, sometimes referred to as the "Theory of Parallel Climate Realizations" (Tel et al., 2019) or the notion of "Contingency" (Gould, 1989), has major implications that call for a reframing of perspective. For example, it means that a single model simulation of the historical period need not match the observed record, even if the model is "perfect" in its physical representation of the real

https://doi.org/10.5194/npg-2022-15
Preprint. Discussion started: 19 October 2022

130 world's climate. However, the statistical characteristics of the model's internal variability must
131 agree with those of the real world, taking into account sampling uncertainty (uncertainty due to
132 limited sampling in the short observational record). Thus, while a single ensemble member need
133 not match observations, the ensemble as a whole should encompass the instrumental data, provided
134 there are enough members to adequately span the range of possible sequences of internal variability
135 (Suarez-Guttierez et al. 2021).
136
137 Another implication of the concept of "parallel climate realizations" is that the climate trends we
138 have experienced are not unique. In analogy with a model LE, the observational record is just one
139 "member" of a larger set of possible "members". Although one cannot replay the "tape of history",
140 one can construct an "Observational LE" by generating alternate synthetic sequences of internal
141 variability from the instrumental data. Conceptually, this involves removing an estimate of the
142 forced component from the data and then randomizing the residual (internal) variability in time.
143 Importantly, the randomization procedure must be done in a way that preserves the statistical
144 properties of the observed variability including its variance, temporal autocorrelation, and spatial
145 patterns. The resulting synthetic sequences of internal variability derived from the observational
146 record can then be added back to the time-evolving forced response obtained from a climate model
147 LE.
148
149 The development of statistically-based Observational LEs is just beginning, with recent efforts
150 targeting surface climate fields (McKinnon et al., 2017; McKinnon and Deser, 2018 and 2021) and
151 carbon dioxide fluxes across the air-sea interface (Olivarez et al. 2022). Here, we focus on the
152 work of McKinnon and Deser (2018 and 2021) who constructed an Observational LE for global

https://doi.org/10.5194/npg-2022-15
Preprint. Discussion started: 19 October 2022


Nonlinear Processes in Geophysics
Discussions
Open Access
EGU

153 sea level pressure (SLP) and terrestrial precipitation and temperature based on ~100 years of
154 monthly gridded instrumental data. To test the skill of their method, they applied it independently
155 to each member of a climate model LE and then compared the results to the "true" statistical
156 properties of the model's internal variability based on the full set of ensemble members. According
157 to this test, their approach was found to be accurate to within 10-20% at most locations. They then
158 constructed a large (1000 member) ensemble of plausible "parallel worlds" of what the
159 observational record might have looked like had a different sequence of internal variability
160 unfolded by chance. Their Observational LE has been used for many applications, including
161 evaluation of internal variability in climate model LEs, assessment of uncertainty in observed 50-
162 year climate trends, and quantification of extreme precipitation risk over the Upper Colorado River
163 basin, a critical water resource for the western US (McKinnon and Deser 2018 and 2021).
164
165 ***d. Dynamical Adjustment***
166 Determining the forced contribution to observed changes in climate remains an ongoing challenge.
167 Most "Detection and Attribution" methods rely on climate models to provide a set of spatial and
168 temporal "fingerprints" of forced climate change that are distinct from patterns of internal
169 variability (Hegerl et al. 2007; Santer et al. 2019; Sippel et al. 2019). These model-based
170 "fingerprints" are then used to assess the proportion of observed climate change that is due to
171 external forcing. However, model shortcomings may limit the accuracy of such methods. Thus, it
172 is also desirable to develop complementary approaches to attribution that do not rely on climate
173 model information. Two such methods, Linear Inverse Modeling (Newman, 2007) and Low-
174 Frequency Pattern Analysis (Wills et al. 2020), leverage the assumption that forced climate change
175 evolves slowly compared to the time scales of internal variability. However, decadal shifts in

https://doi.org/10.5194/npg-2022-15
Preprint. Discussion started: 19 October 2022

regional anthropogenic aerosol emissions during the industrial era present challenges to this assumption and may complicate interpretation of the results (Deser et al. 2020; Persad et al. 2018).

A complementary, physically-based approach to isolating the externally-forced response in observations without reliance on climate model information is the technique of "Dynamical Adjustment". This method aims to remove the influence of atmospheric circulation variability from surface climate anomalies, thereby revealing the thermodynamically-induced component of observed climate change (Wallace et al. 2013; Smoliak et al. 2015; Deser et al. 2016). According to the current generation of coupled climate models, the forced component of extra-tropical atmospheric circulation changes is small relative to internal variability (Deser et al. 2012; Shepherd, 2014). If models are correct in this regard, then dynamical adjustment can be used to parse the relative contributions of internal dynamics and forced thermodynamics to observed climate changes at middle and high latitudes (Wallace et al. 2013; Deser et al. 2016). A variety of dynamical adjustment algorithms have been developed and tested within the framework of a model LE (Deser et al., 2016; Lehner et al., 2017 and 2018; Smoliak et al., 2015; Guo et al. 2019; Merrifield et al., 2017; Terray 2021; Sippel et al. 2019). These protocols are all based on statistical associations between patterns of SLP and surface climate anomalies deduced from long observational records. Generally, the data are high-pass filtered or detrended so as to avoid aliasing any potential forced component onto the statistical relationships. These procedures generally work best for large-amplitude SLP anomaly patterns, and are more effective for temperature than precipitation due to higher levels of noise in the latter (Guo et al. 2019).

2. Data and Methods

https://doi.org/10.5194/npg-2022-15
Preprint. Discussion started: 19 October 2022

We make use of a state-of-the-art 100-member LE conducted with the National Center for Atmospheric Research (NCAR) Community Earth System Model version 2 (CESM2), described in Rodgers et al. (2021). This publicly-available LE resource is unprecedented for its combination of large ensemble size, high spatial resolution (approximately 1° in both latitude and longitude), and length of simulation (1850-2100). Each ensemble member is driven by the same radiative forcing scenario (historical from 1850-2014, and SSP3-7.0 from 2015-2100), but begins from a different state on 1 January 1850, taken from a long pre-industrial control simulation. We analyze linear trends over the past 50 years (1972-2021) and projected for the next 50 years (2022-2071). It should be noted that memory of the initial state is negligible by the middle of the 20th century; thus, diversity in trends amongst the individual ensemble members is solely due to different random samples of internal variability, which are superimposed upon a common forced response.

For consistency with the 100-member CESM2 LE, we make use of the first 100 members of the Observational LE (OBS LE) constructed by McKinnon and Deser (2018) to illustrate the diversity of past 50-year trends consistent with the statistical spatio-temporal properties of internal variability in the observational record. For the purpose of comparing directly to the CESM2 LE, we have added the model's forced trend to the internal trend of each OBS LE member. The OBS LE is based on the Berkeley Earth Surface Temperature (BEST) dataset (Rohde et al. 2013), the Global Precipitation Climatology Centre (GPCC) dataset (Schneider et al. 2008), and the Twentieth Century Reanalysis version 2c (20CR) sea level pressure (SLP) dataset (Compo et al. 2011).

https://doi.org/10.5194/npg-2022-15
Preprint. Discussion started: 19 October 2022


Nonlinear Processes in Geophysics Discussions
Open Access
EGU

We apply the dynamical adjustment methodology of Deser et al. (2016) based on SLP "constructed circulation analogues" to monthly temperature and precipitation during 1900-2021, using the same observational data sets as in the OBS LE. The reader is referred to Deser et al. (2016) for details of the methodology, and to Lehner et al. (2017 and 2018), Guo et al. (2019) and Terray (2021) for additional applications.

For each ensemble member of the CESM2 and OBS LEs, we form monthly anomalies by subtracting the long-term means for each month individually, and then form seasonal averages (December-February) of the monthly anomalies. We compute 50-year trends of the wintertime anomalies using linear least-squares regression analysis. All results shown in this study are original findings.

3. European climate trends

We begin by illustrating the diversity of winter temperature and precipitation trends over Europe during the past 50 years (1972-2021) in the CESM2 and OBS LEs (Sections 3a and b), and projected for the next 50 years (2022-2071) in the CESM2 LE (Section 3c). We then provide a more quantitative view of the relative contributions of forced climate change and internal variability to past and future climate trends using a variety of signal-to-noise metrics, with comparison between the CESM2 and OBS LEs (Section 3d). We summarize the CESM2 LE results by showing the "expected range" of trend outcomes in Section 3e. Finally, we apply the technique of "dynamical adjustment" to estimate the forced component of observed temperature trends (Section 3f), and then use this estimate in conjunction with the OBS LE to produce a purely

https://doi.org/10.5194/npg-2022-15
Preprint. Discussion started: 19 October 2022


Nonlinear Processes in Geophysics Discussions

243 observational estimate of the plausible range of temperature trend outcomes over the past 60 years
244 (Section 3g).
245
246 ***a. Past trends (1972-2021) in the CESM2 LE***
247 The CESM2 model simulates a wide range of wintertime temperature trend patterns for the past
248 50 years due to the combined effects of internal variability and forced response, as illustrated by
249 the first 28 members of the LE (Fig. 1). Recall that the only reason that these trend maps are not
250 identical is because of random differences in internal variability between the members. While
251 moderate warming is seen over most of the European continent in the majority of cases, as
252 expected, some members show regions of considerably greater temperature increase (in excess of
253 1°C per decade for example members 1, 10 and 18), while others exhibit weak cooling in some
254 locations (for example, members 17, 23 and 26; Fig. 1). The relative contributions of internal
255 variability and forced response can be readily discerned by comparing the individual member
256 trends with the ensemble-mean trend (see "EM" panel in Fig. 1). The observed trend ("OBS"
257 panel in Fig. 1) bears a close resemblance to the model's forced trend in both amplitude and spatial
258 pattern. This correspondence may be coincidental, as individual members of the CESM2 LE also
259 resemble the forced response (for example, members 6 and 21), or it may suggest that the model
260 overestimates the amplitude of internally-generated 50-year trends relative to forced trends. The
261 OBS LE results shown below will shed some light on these two possibilities.

https://doi.org/10.5194/npg-2022-15
Preprint. Discussion started: 19 October 2022

Nonlinear Processes in Geophysics
Discussions
Open Access
EGU

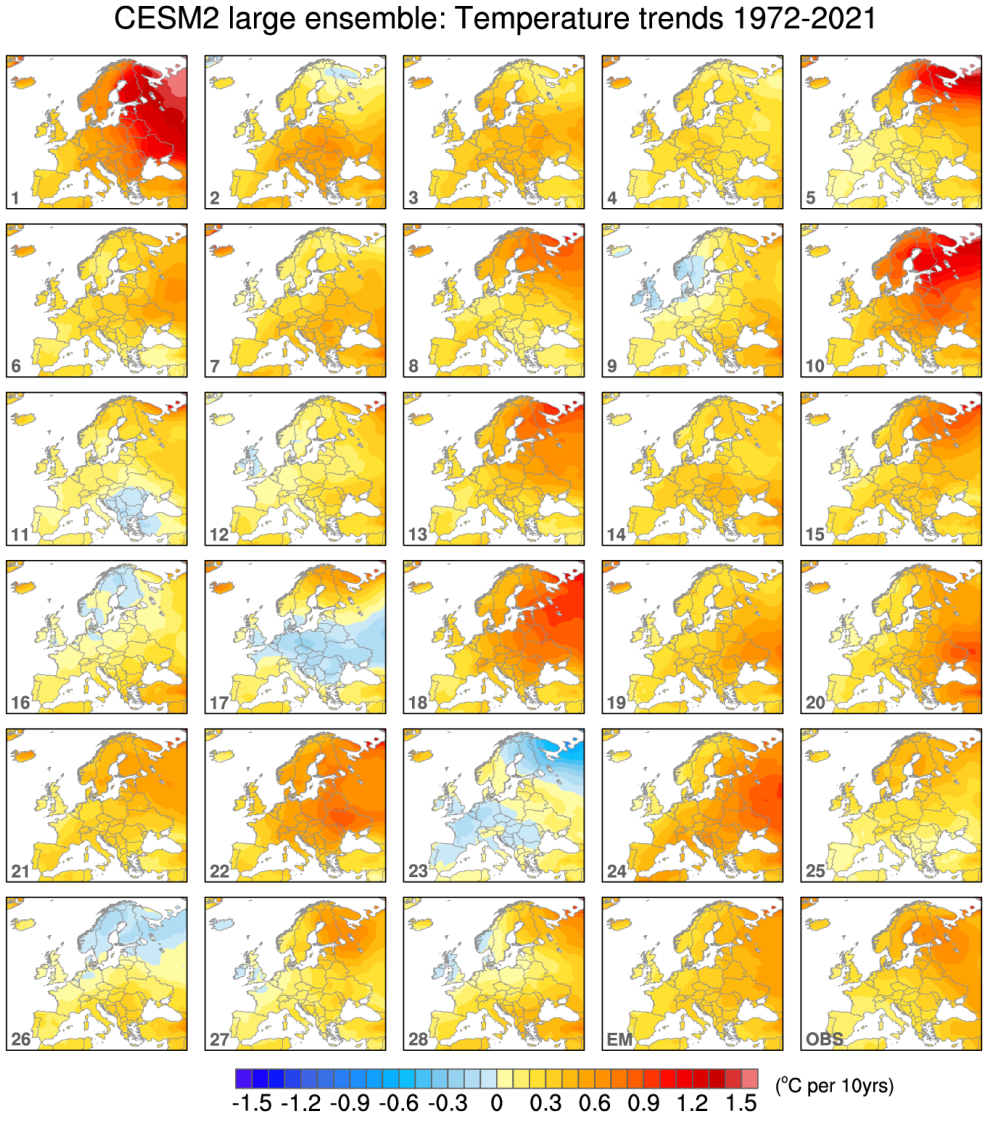

Figure 1. Winter air temperature trends (°C per decade) for the period 1972-2021 as simulated by the first 28 members of the CESM2 Large Ensemble (number in the lower left of each panel denotes the ensemble member) and the 100-member ensemble-mean (panel labeled "EM"). Observed trends are shown in the lower right (panel labeled "OBS").

https://doi.org/10.5194/npg-2022-15
Preprint. Discussion started: 19 October 2022

Nonlinear Processes in Geophysics
Discussions
Open Access
EGU

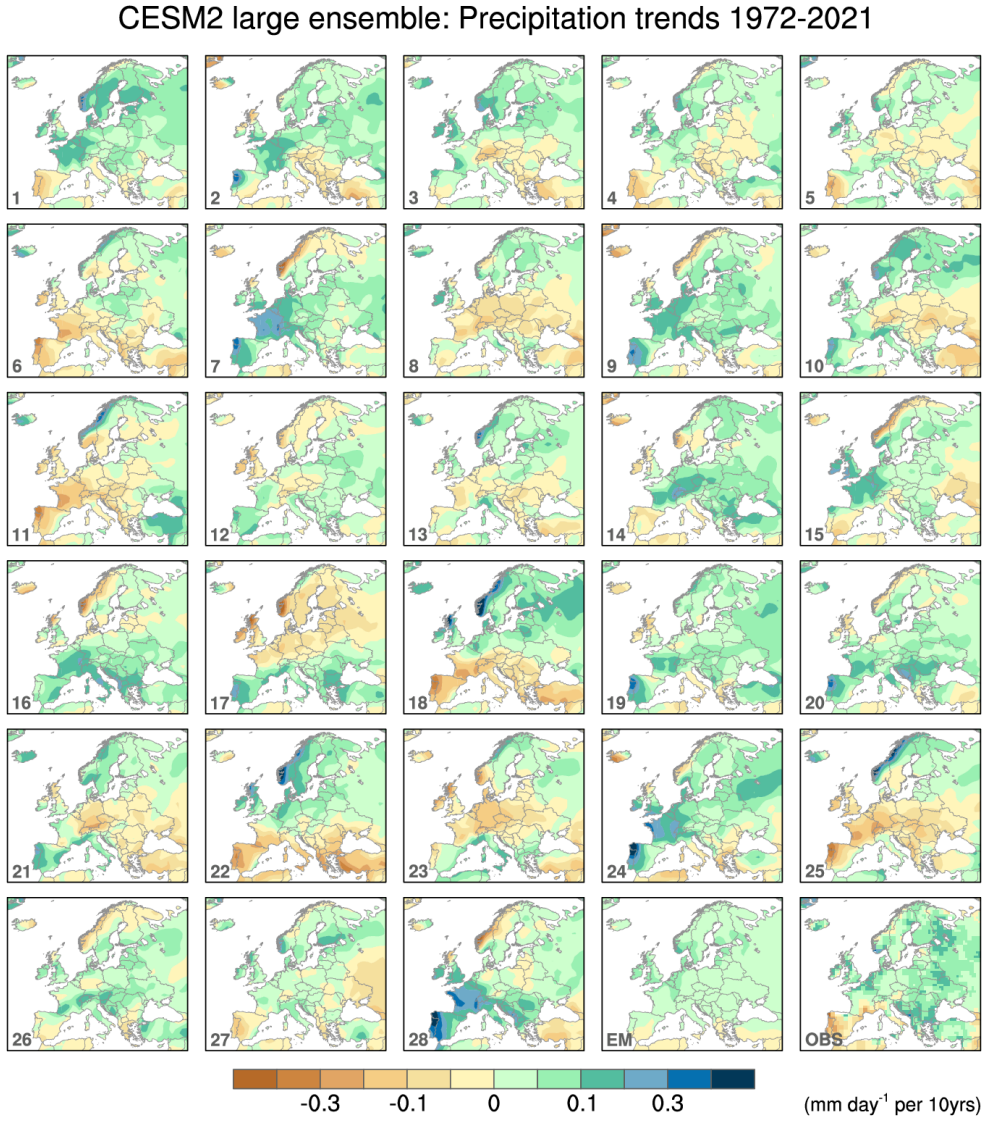

Figure 2. As in Fig. 1 but for precipitation (mm d-1 per decade).

Like temperature, precipitation trends also vary considerably across ensemble members (Fig. 2). While the ensemble-mean trend shows modest increases in precipitation throughout Europe (except for the southernmost fringes), internal variability can evidently overwhelm the forced response in individual simulations. For example, some members show drying over large parts of

https://doi.org/10.5194/npg-2022-15
Preprint. Discussion started: 19 October 2022

the continent, while others depict enhanced wetting in the same regions (compare, for example, members 22 and 28, which show nearly opposite patterns). Observed precipitation trends are generally positive, except over Spain, Portugal, southern France and other parts of the western Mediterranean (Fig. 2). The observed precipitation increases, while of the same sign as the model's forced response, are approximately twice as large in many areas. Again, the interpretation of the observed trends is ambiguous, since there are individual members that resemble observations (for example, member 1).

b. Past trends (1972-2021) in the OBS LE

The individual members of the OBS LE show a qualitatively similar diversity of 50-year temperature trends as the CESM2 LE (Fig. 3). Like CESM2, some members show weak cooling in some areas while others show widespread moderate or strong warming. This suggests that the resemblance between the observed trend and the model's forced response may be purely coincidental. Precipitation trends in the OBS LE also display large contrasts between members, similar to CESM2 (Fig. 4). For example, nearly opposite patterns are found between members 6 and 11 (or 8 and 9). Trend amplitudes also vary considerably across the OBS LE, with larger magnitudes in some members (for example, members 3 and 20) compared to others (e.g., members 21 and 13). While no single member of the 28 OBS LE samples shown matches the model's forced trend, member 21 with its relatively muted trends comes close.

https://doi.org/10.5194/npg-2022-15
Preprint. Discussion started: 19 October 2022

Nonlinear Processes in Geophysics
Discussions
Open Access
EGU

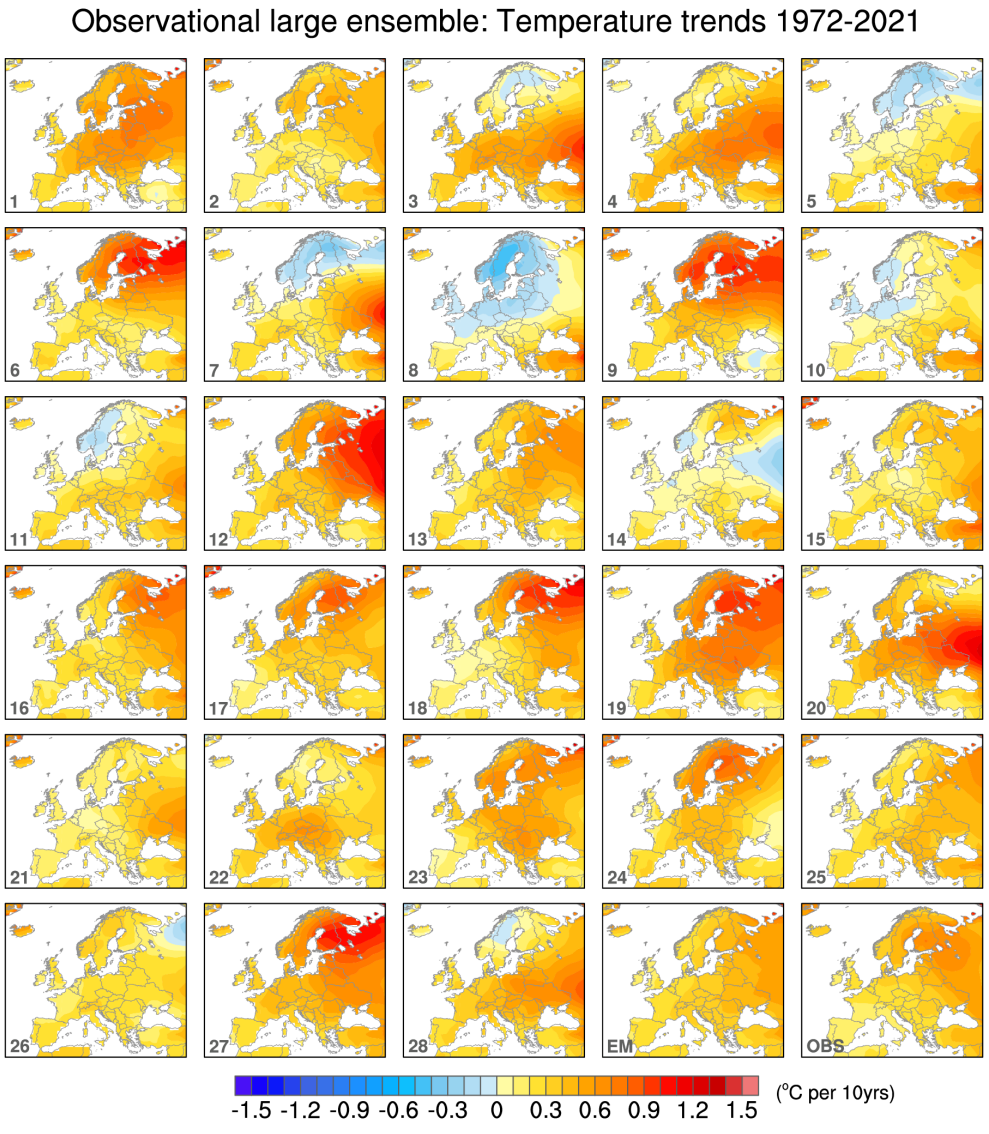

294

295 **Figure 3.** As in Fig. 1, but for the Observational Large Ensemble of McKinnon and Deser (2018)
296 with the ensemble-mean from the 100-member CESM2 Large Ensemble. See text for details.
297

https://doi.org/10.5194/npg-2022-15
Preprint. Discussion started: 19 October 2022

Nonlinear Processes in Geophysics
Discussions
Open Access
EGU

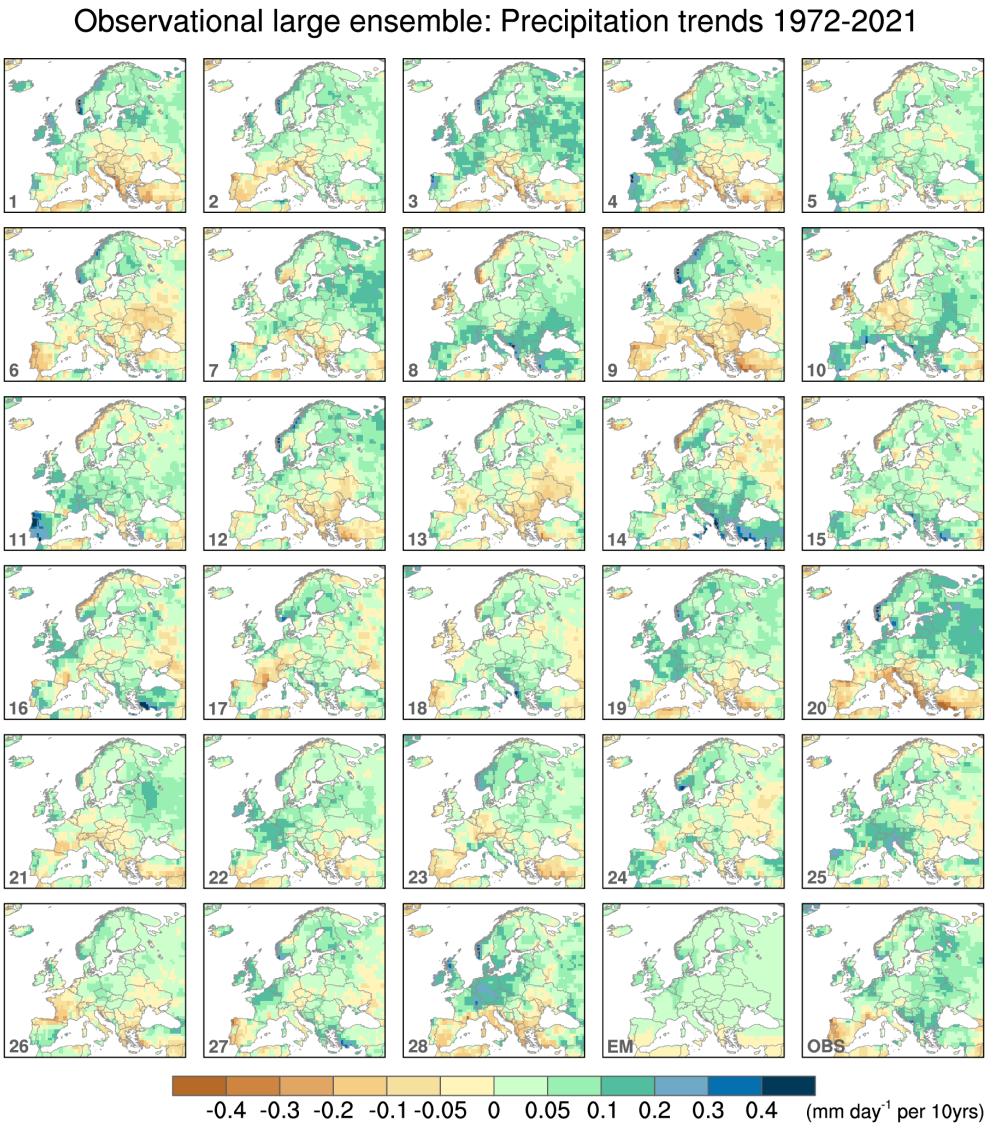

298

299 **Figure 4.** As in Fig. 2, but for the Observational Large Ensemble of McKinnon and Deser (2018)
300 with the ensemble-mean from the 100-member CESM2 Large Ensemble. See text for details.
301

https://doi.org/10.5194/npg-2022-15
Preprint. Discussion started: 19 October 2022


Nonlinear Processes in Geophysics Discussions

c. Future Trends (2022-2071) in the CESM2 LE

As expected, temperature trends projected for the next 50 years show larger amplitudes than those for the past 50 years in the CESM2 LE (Fig. 5). This is due to the fact that the forced (ensemble-mean) component of warming increases as greenhouse gas emissions accelerate. In most regions, the forced warming trend increases by approximately 0.2°C per decade in the future compared to the past. Notable exceptions are Iceland and the British Isles, which show less warming in the future due to a circulation-induced forced cooling trend (see Section 3e). Despite a larger forced component, temperature trends projected for the next 50 years still show a wide range of amplitudes across individual members of the CESM2 LE. For example, member 13 is striking for its muted warming (generally < 0.5°C per decade) across Europe (and absolute cooling over the UK and Iceland), while member 28 shows highly amplified warming, with values exceeding 1.3 °C per decade over western Russia.

Forced trends in precipitation are projected to amplify over the next 50 years, with greater wetting over northern Europe and drying over southern Europe and the Mediterranean (Fig. 6). In addition, the region with a forced drying trend is projected to expand northward into Spain, Italy and the Balkan Republics. While the forced pattern of future drying in the south and wetting in the north is generally evident in most of the simulations shown, there are notable differences in amplitude across the members. For example, member 28 shows precipitation trends in excess of 0.1 mm d^{-1} per decade over most of northern Europe, while member 11 shows positive precipitation trends of less than half this amount. Members 27 and 28 illustrate that the mid-section of the European continent may get wetter or drier depending on the unpredictable sequence of internal variability

https://doi.org/10.5194/npg-2022-15
Preprint. Discussion started: 19 October 2022

Nonlinear Processes in Geophysics
Discussions
Open Access
EGU

324 that unfolds. Thus, internal variability can still make a sizeable contribution to the projected
325 patterns and amplitudes of winter precipitation trends over the next 50 years.

326

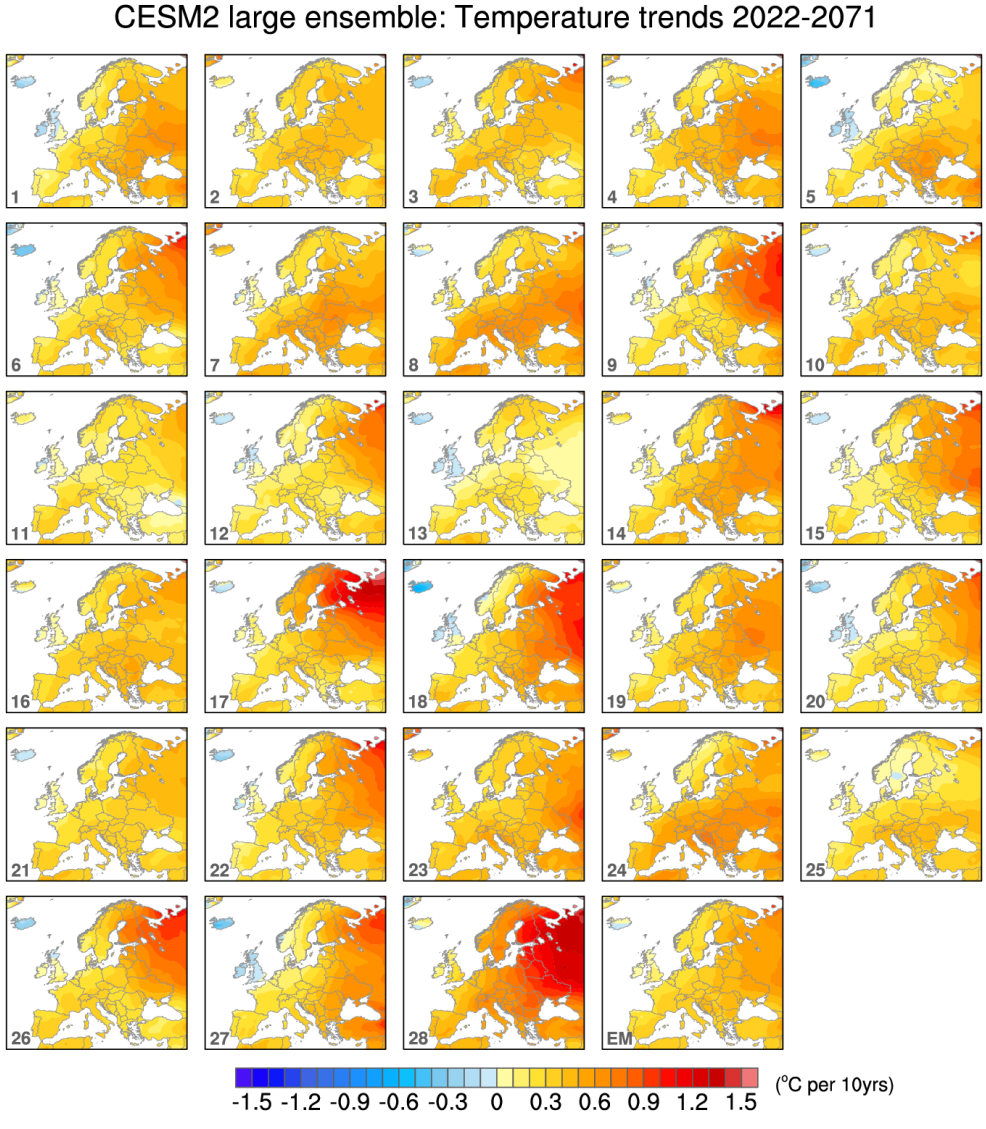

327

328 **Figure 5**. As in Fig. 1, but for the period 2022-2071.
329
330

https://doi.org/10.5194/npg-2022-15
Preprint. Discussion started: 19 October 2022

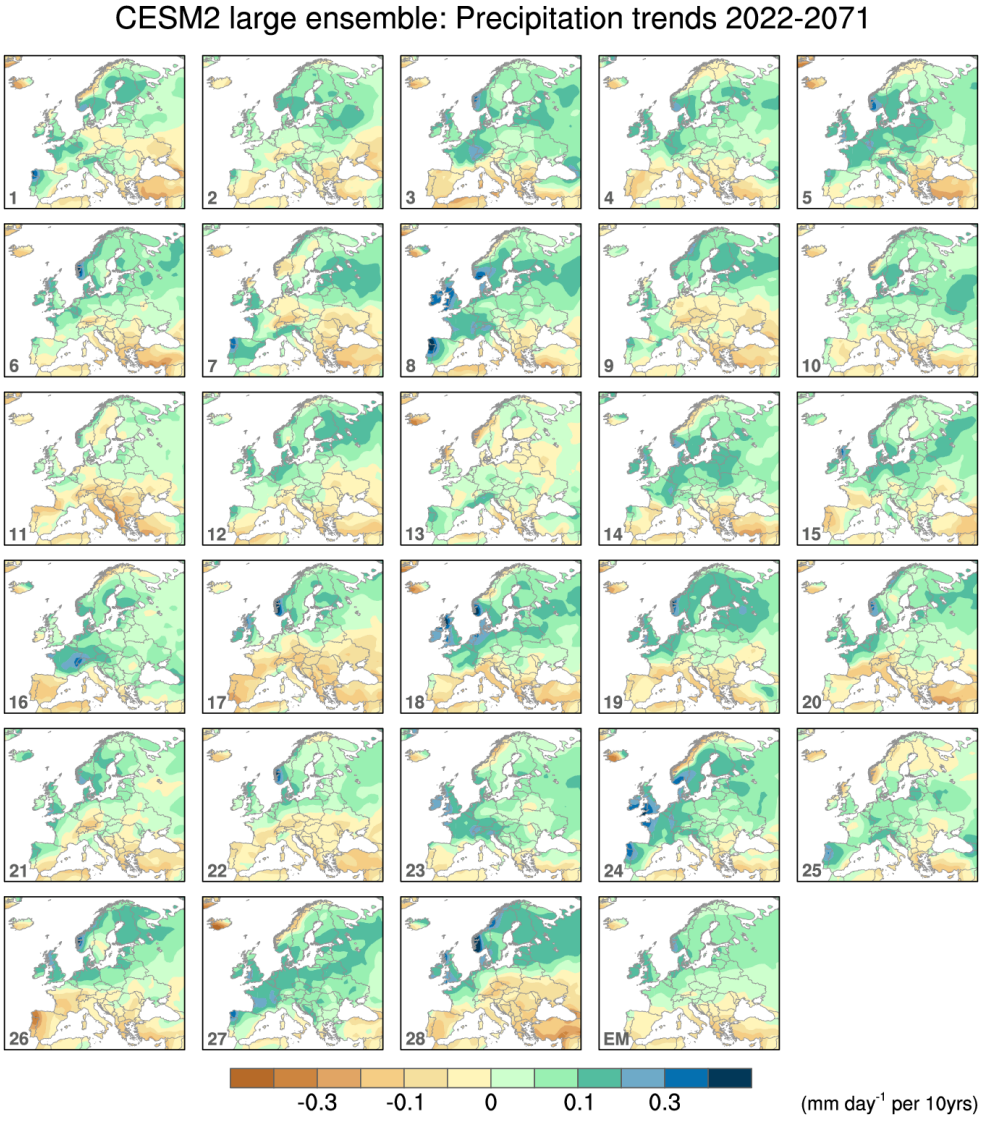

Figure 6. As in Fig. 2, but for the period 2022-2071.

https://doi.org/10.5194/npg-2022-15
Preprint. Discussion started: 19 October 2022


Nonlinear Processes in Geophysics
Discussions
Open Access
EGU

d. Signal-to-noise metrics and model evaluation.

In the previous section, we conveyed a qualitative impression of the possible range of 50-year trends due to the superposition of internal variability and forced climate change in the CESM2 and OBS LEs. Here, we provide a more quantitative view, beginning with a comparison of the standard deviation (σ) of trends over the period 1972-2021 computed across the ensemble members of each LE. In the CESM2 LE, the ensemble σ of temperature trends increases from southwest to northeast, with minimum values (0.05-0.10 K per decade) over Spain and northern Africa, and maximum values (0.30-0.35 0.5°C per decade) over northwestern Russia (Fig. 7a). A similar pattern is found in OBS LE, with some regional differences in amplitude (Fig. 7b). In particular, the ensemble σ values are significantly smaller (20-40%) over Scandinavia, Germany and Poland, and significantly larger (20-40%) in areas near the Mediterranean and Black Seas, in the OBS LE compared to the CESM2 LE (Fig. 7c). For precipitation trends, the two LEs show similar patterns of ensemble σ, with largest amplitudes generally along the west coasts (0.10 - 0.25 mm d^{-1} per decade) and over southwestern Europe (values 0.05 – 0.10 mm d^{-1} per decade: Figs. 7d and e). However, CESM2 LE significantly underestimates the OBS LE by more than 40% along the Mediterranean and Black Seas and parts of Russia, and significantly overestimates the OBS LE by 20-40% in many areas of western Europe (Fig. 7f).

https://doi.org/10.5194/npg-2022-15
Preprint. Discussion started: 19 October 2022

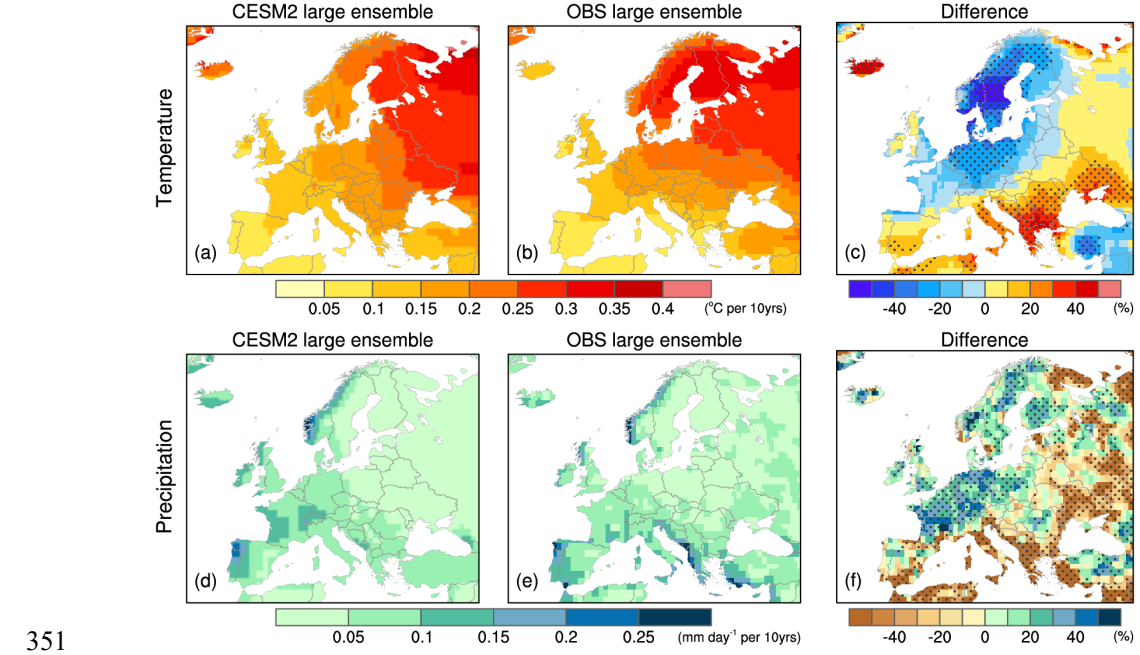

Figure 7. Standard deviation of 50-year trends (1972-2021) across 100 members of the CESM2 Large Ensemble (a,d) and 100 members of the Observational Large Ensemble (b,e), and their difference (c,f) for winter air temperature (top; °C per decade) and precipitation (bottom; mm d^{-1} per decade). Stippling in panels c and f indicates that the differences are statistically significantly at the 95% confidence level.

Next, we assess the relative magnitude of the forced and internal components of trends by computing a "signal-to-noise" ratio defined as the CESM2 ensemble-mean trend divided by the σ of trends across the 100 members of each LE. This "signal-to-noise" ratio indicates whether the forced trend can be readily detected in any single ensemble member (and by extension, the real world), or whether internal variability dominates. For a normal distribution, a signal-to-noise ratio greater than two indicates that the ensemble-mean (forced) trend is significantly different from zero at the 95% confidence level: that is, there is less than a 5% chance that the ensemble-mean trend could have been a result of random internal variability. In CESM2, the signal-to-noise of forced temperature trends over the past 50 years generally ranges from 1.5 - 2 over central and

https://doi.org/10.5194/npg-2022-15
Preprint. Discussion started: 19 October 2022

Nonlinear Processes in Geophysics
Discussions
Open Access
EGU

northern Europe, and from 2-3 over southern Europe (Fig. 8a). Forced precipitation trends over the past 50 years exhibit much lower signal-to-noise ratios than temperature, with values generally < 1 and nearly always < 1.5 (Fig. 8d).

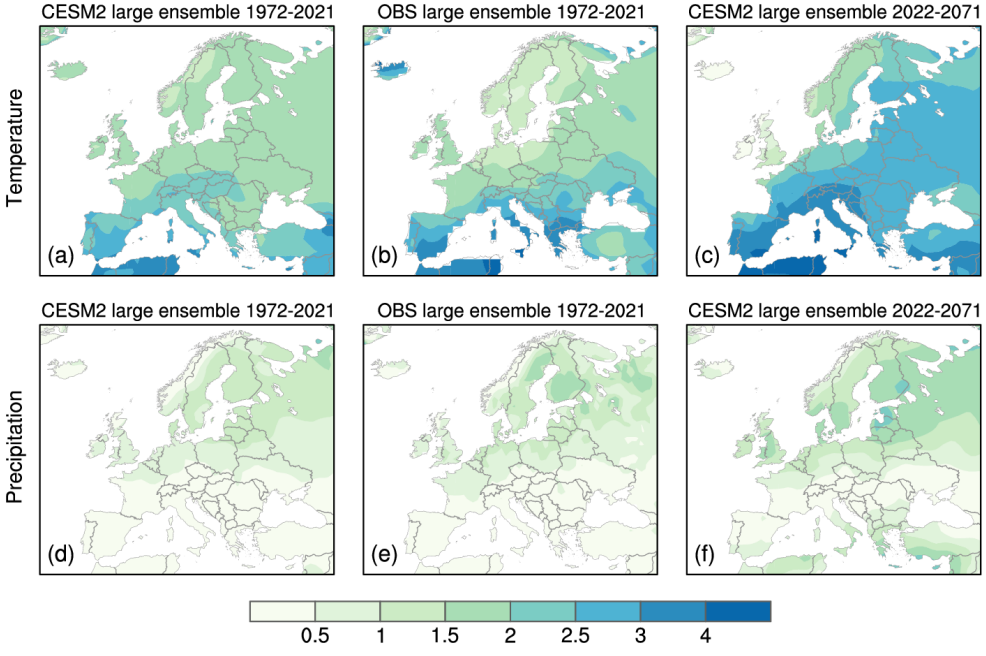

Figure 8. Signal-to-noise of forced trends in winter (top) air temperature and (bottom) precipitation based on the 100-member CESM2 Large Ensemble during 1972-2021 (a,d), the Observational Large Ensemble during 1972-2021 (b,e), and the CESM2 Large Ensemble during 2022-2071 (c,f). See text for details.

How much do model biases in ensemble σ shown previously affect the signal-to-noise of the model's forced trends? We address this question by using the OBS LE σ values in place of the model's σ values in the signal-to-noise calculation. This substitution results in an enhancement of signal-to-noise of past forced temperature trends over southern Europe and a reduction in signal-to-noise over Scandinavia, Germany and Poland, with a net increase from 38% to 60% in the area with values > 2 (Fig. 8b). The impact of model biases in ensemble trend σ is much less pronounced

https://doi.org/10.5194/npg-2022-15
Preprint. Discussion started: 19 October 2022

382 for precipitation than temperature, with signal-to-noise values in all locations remaining below 2
383 (Fig. 8e).
384
385 As expected, signal-to-noise values are higher for forced trends in the future than in the past.
386 Ninety-seven percent of the area of the continent (excluding Iceland and Greenland) shows a
387 signal-to-noise value > 2 for forced temperature trends during 2022-2071 (Fig. 8c), compared with
388 38% for trends during 1972-2021. Forced precipitation trends in the future remain uncertain, with
389 only 2% of the land area showing a signal-to-noise value > 2 (Fig. 8f).
390
391 Another way to view the relative impacts of internal variability and external forcing on trends is
392 by computing the fraction of ensemble members at each location that show a positive trend (e.g.,
393 warming or wetting). This metric conveys the likelihood of having a positive (or negative) trend
394 in any single ensemble member, which is analogous to the single "realization" of the real world.
395 At nearly all locations, more than 95% of ensemble members in the CESM2 LE show warming in
396 both the past and future periods, with slightly lower percentages (85-95%) over western
397 Scandinavia and parts of Great Britain (and < 75% over Ireland, Scotland and Iceland in the
398 future); (Figs. 9a and c). Similar percentages are obtained when the internal component of past
399 temperature trends in the OBS LE is used in place of the model's internal trends, with some
400 reduction (75-95%) over Scandinavia, northern Russia, Germany and Poland (Fig. 9b).

https://doi.org/10.5194/npg-2022-15
Preprint. Discussion started: 19 October 2022

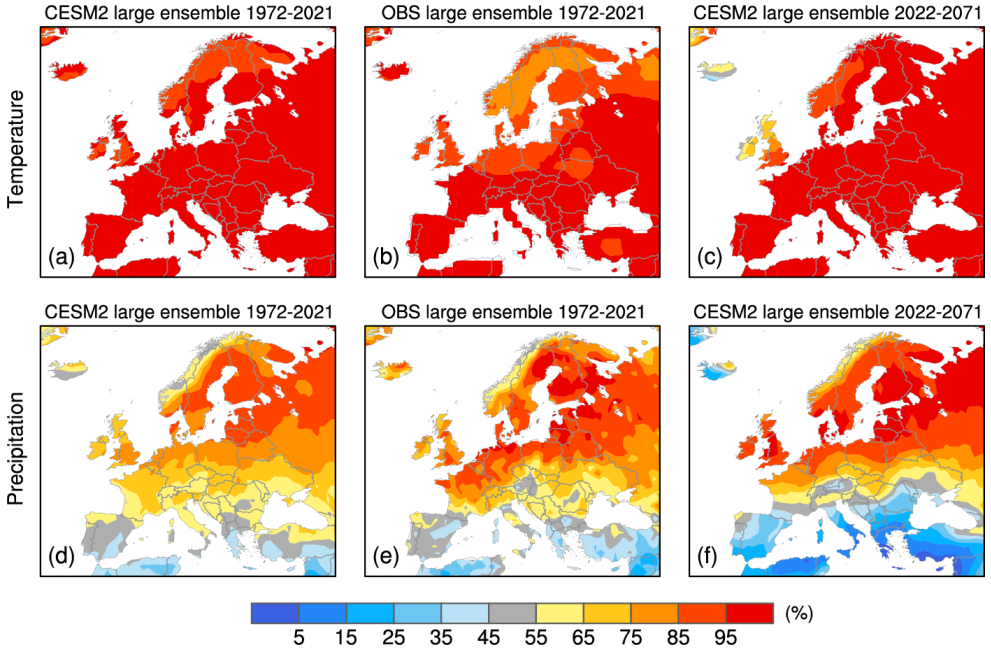

401

402 **Figure 9**. The percentage of ensemble members with a positive trend in winter (top) air
403 temperature and (bottom) precipitation trends based on (a,d) the 100-member CESM2 Large
404 Ensemble during 1972-2021, (b,e) the 100-member Observational Large Ensemble during 1972-
405 2021, and (c,f) the 100-member CESM2 Large Ensemble during 2022-2071.
406

407 The sign of the trend in any given ensemble member is more uncertain for precipitation than for
408 temperature. The highest chances (> 85%) of a positive precipitation trend are found over the
409 northernmost third of the continent excluding Norway, both in the past and future (Figs. 9d and f).
410 Similarly high chances of a negative precipitation trend (equivalent to < 15% of a positive trend)
411 occur in areas near the Mediterranean Sea, but only in the future. The central portion of the
412 continent shows roughly equal chances of having a positive or negative trend, both in the past and
413 future. The area with a > 85% chance of a positive precipitation trend in the past 50 years expands
414 southward into northern France, Germany and areas bordering the Baltic Sea when internal
415 variability is derived from the OBS LE compared to the CESM2 LE (Fig. 9e).
416

https://doi.org/10.5194/npg-2022-15
Preprint. Discussion started: 19 October 2022

417 Taken together, the results shown in Fig. 9 indicate that warming is virtually guaranteed at nearly
418 all locations, both in the past 50 years and the next 50 years, according to the CESM2 LE.
419 However, the sign of the precipitation trend (past and future) is robust only over the northern tier
420 of the continent, and only in the future over the Mediterranean region. The model results for past
421 trends are found to be generally credible as measured against the OBS LE, with some
422 overestimation in north-central Europe.
423
424 ***e. Range of outcomes and the role of the atmospheric circulation***
425 As the saying goes, "climate is what we expect, weather is what we get". This adage is also
426 applicable to climate change, where "human-induced climate change is what we expect, internal
427 variability plus human-induced climate change is what we get" (Deser 2020). Here, we illustrate
428 "what we expect" and the range of "what we get" for past and future 50-year trends in the CESM2
429 LE, using the ensemble-mean for "what we expect" and two contrasting ensemble members for
430 the range of "what we get". We select the contrasting members from the bottom and top 5th
431 percentiles of the distribution of 100-member trends averaged over the European continent for
432 each period separately. This selection criterion is somewhat arbitrary and does not necessarily
433 capture the wide range of trend amplitudes that may occur at a single location or sub-region, nor
434 does it portray the full range of spatial patterns that occur within the ensemble.
435
436 There is a large range in temperature trend outcomes ("what we get") for both the past 50 years
437 and the next 50 years as depicted by the "warm" and "cool" end-members (Fig. 10). For past
438 trends, the "warm" end-member shows temperature increases of 0.9-1.1 °C per decade over the
439 eastern portion of the continent (Fig. 10b), while the "cool" end-member displays muted warming

https://doi.org/10.5194/npg-2022-15
Preprint. Discussion started: 19 October 2022

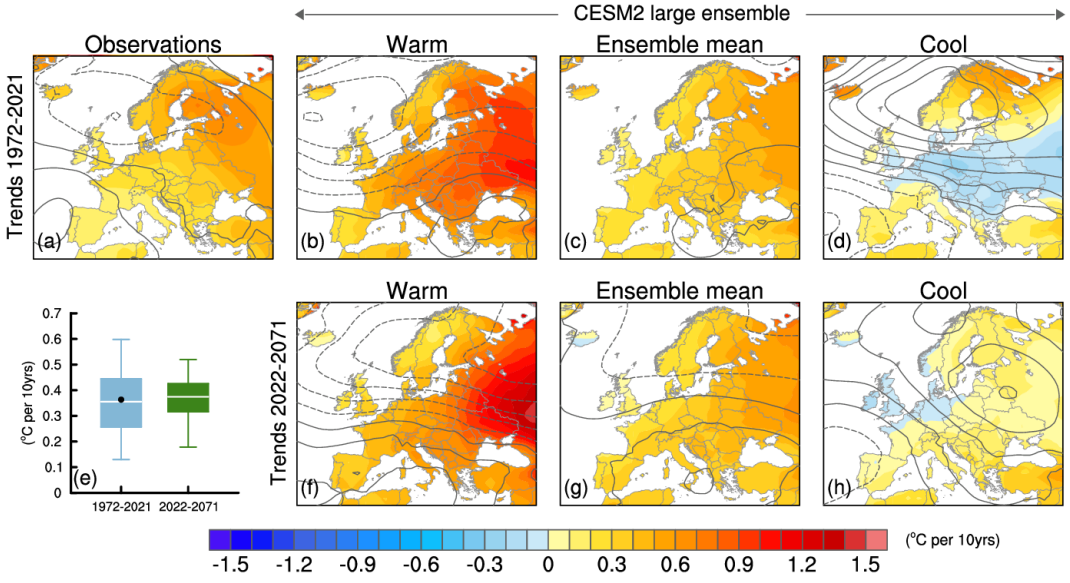

Figure 10. **A Range of Outcomes.** Trends in winter air temperature (color shading; °C per decade) and sea-level pressure (SLP) (contours; contour interval of 0.25 hPa per decade, negative values dashed) for the period (top) 1972-2021 and (bottom) 2022-2071. Panel (a) shows observed trends (1972-2021) and remaining panels show simulated trends from the 100-member CESM2 Large Ensemble: (c,g) ensemble-mean; (b,f) "warm" end-member; (d,h): "cool" end-member. See text for details. Panel (e): Distribution of European-average trends for 1972-2021 (blue) and 2022-2071 (green) from the CESM2 Large Ensemble (box outlines 25th-to-75th percentile range, whiskers mark the 5th-to-95th percentile range, the horizontal white line denotes the median value, and the black circle marks the observed value).

(< 0.3 °C per decade) and even slight cooling through the midsection of the continent (Fig. 10d). Clearly, the forced trend ("what we expect"), which depicts moderate warming (0.2-0.6°C per decade) across the continent does not tell the whole story (Fig. 10c). Analogous results are found for trends projected over the next 50 years: the "warm" member shows temperature increases of 1.0-1.5 °C per decade over west-central Russia (Fig. 10f) while the "cool" member depicts < 0.2°C per decade warming over most of the continent (Fig. 10h), in marked contrast to the forced trend which ranges from 0.3-0.6°C per decade (Fig. 10g). As discussed previously, the observed temperature trend map resembles the model's ensemble-mean, but this could be by chance (Fig.

https://doi.org/10.5194/npg-2022-15
Preprint. Discussion started: 19 October 2022

459 10a). In terms of European averages, the observed trend (0.36 °C per decade) is nearly coincident
460 with the median value of the model's trend distribution, which has a 5th-to-95th percentile range of
461 0.13-0.60 °C per decade for past 50-year trends (Fig. 10e). Curiously, the model's median trend
462 value for Europe as a whole increases only slightly in the future compared to the past, while the
463 5th-to-95th percentile range narrows slightly (Fig. 10e). Further work is needed to understand why
464 this is the case.
465
466 As mentioned in Section 1d, previous work has shown that internal variability of the large-scale
467 atmospheric circulation causes much of the member-to-member differences in temperature trends
468 in model LEs. Here, we provide a qualitative indication of the circulation influence by
469 superimposing SLP trends upon the maps in Fig. 10. In the case of past trends, the "warm" member
470 shows a positive North Atlantic Oscillation (NAO)-like pattern (Hurrell et al. 2003), with negative
471 SLP trends centered near Iceland and positive SLP trends centered over the Mediterranean (Fig.
472 10b). This SLP pattern is indicative of stronger westerly/southwesterly flow, which brings
473 relatively warm maritime air over the continent. The "cool" member shows a largely opposite
474 flow configuration (albeit with longitudinal shifts in the SLP centers-of-action), which advects
475 relatively cold air from the east over the continent (Fig. 10d). In comparison, the forced response
476 shows negligible atmospheric circulation change (Fig. 10c). Striking contrasts in circulation are
477 also found for the future period, with a large positive NAO-like trend pattern in the "warm"
478 member and a blocking continental "High" in the "cool" member (Figs. 10f and h). Future trends
479 in SLP also contain a modest forced component indicative of enhanced westerlies over the
480 continent (Fig. 10g).
481

https://doi.org/10.5194/npg-2022-15
Preprint. Discussion started: 19 October 2022

Nonlinear Processes in Geophysics
Discussions
Open Access
EGU

482 The "wet" and "dry" end-members also show striking regional contrasts in both precipitation and
483 circulation (Fig. 11). For example, for past trends, the "wet" member shows precipitation increases
484 of 0.2-0.3 mm d^{-1} per decade over France, southern Germany, Portugal and the UK, and
485 precipitation declines over northern Norway and along the Mediterranean Sea (Fig. 11b). A nearly
486 opposite pattern is found for the "dry" member (Fig. 11d). These contrasting precipitation trends
487 can be understood in the context of the overlying atmospheric circulation changes, with wetter
488 areas coinciding with anomalous westerly/southwesterly flow and drier areas located under
489 blocking anticyclones. Analogous patterns are found for future trends, with pronounced increases
490 in precipitation over western Europe associated with the low pressure trend centered over the
491 British Isles in the "wet" member (Fig. 11f), and generally reduced precipitation in the "dry"
492 member associated with the blocking High centered over southern Europe (Fig. 11h).

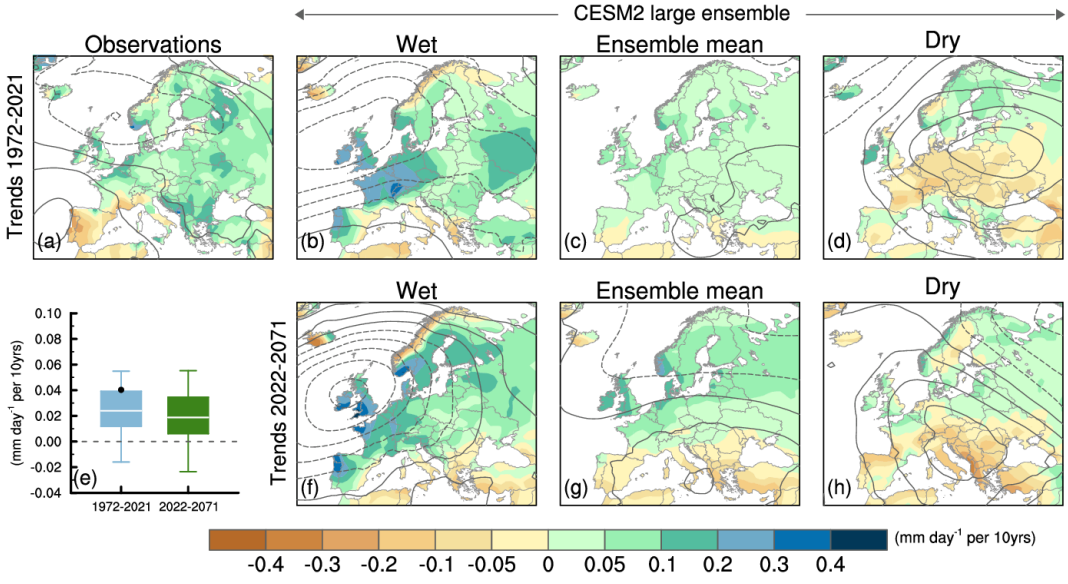

493

494 **Figure 11**. As in Fig. 10 but for precipitation (mm d^{-1} per decade).
495

https://doi.org/10.5194/npg-2022-15
Preprint. Discussion started: 19 October 2022


Nonlinear Processes in Geophysics
Discussions
Open Access
EGU

496

497 ***f. Unmasking forced climate change in observations via "Dynamical Adjustment"***

498 The empirical method of "dynamical adjustment" introduced in Section 1d can be used to estimate
499 the circulation-induced component of observed temperature anomalies; this dynamically-induced
500 contribution can then be subtracted from the original anomaly to obtain the thermodynamically-
501 induced component as a residual. Since this method uses no information from climate models, it
502 provides an independent estimate of the thermodynamic component of observed temperature
503 trends, which can be compared with the forced response simulated by climate model LEs.

504

505 Figure 12 shows the decomposition of observed DJF temperature trends into their dynamical and
506 residual thermodynamic contributions. For this example, we have used the 60-year period 1962-
507 2021 when observed SLP trends are more than twice as large as those during 1972-2021 on a per
508 decade basis (compare SLP contours in Figs. 10a and 12a). Observed SLP trends during the past
509 60 years show a pronounced positive NAO-like pattern, with maximum negative values of -1.25
510 hPa per decade near Iceland and maximum positive values of +0.75 hPa per decade west of Spain
511 (Fig. 12a). Enhanced westerly/southwesterly flow associated with this pattern advects warm air,
512 raising surface temperatures by 0.1- 0.3°C per decade (with maximum warming over northern
513 Europe) according to the dynamical adjustment algorithm (Fig. 12b). Removing this dynamically-
514 induced component from the total trend reveals the residual thermodynamic contribution to the
515 observed warming trend (Fig. 12c). This observed thermodynamic trend is much closer in
516 amplitude (and arguably pattern) to the model's forced response, given by the CESM2 LE
517 ensemble-mean trend (Fig. 12d), than is the total observed trend. Further, the lack of an
518 appreciable forced SLP trend in CESM2 indicates that the model's forced temperature trend is

https://doi.org/10.5194/npg-2022-15
Preprint. Discussion started: 19 October 2022

Nonlinear Processes in Geophysics
Discussions
Open Access
EGU

519 thermodynamically-driven. The level of agreement between the observed thermodynamic
520 temperature trend and the model's forced thermodynamic trend leads to two powerful conclusions:
521 1) the model's forced temperature trend is realistic; and 2) removing the circulation-induced
522 component from the observed trends can effectively reveal the influence of anthropogenic forcing.
523 Analogous results have been found for North America (Deser et al. 2016).

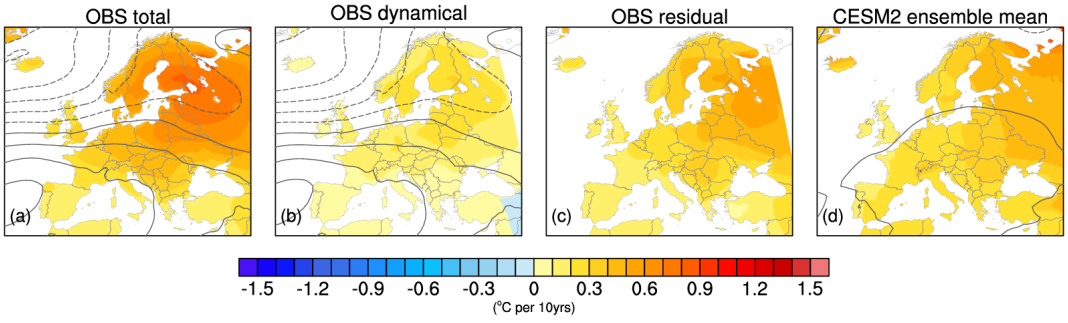

524

525 **Figure 12**. Decomposition of (a) observed winter air temperature trends (1962-2021; °C per
526 decade) into (b) dynamical and (c) residual thermodynamic contributions using the "dynamical
527 adjustment" procedure of Deser et al. (2018) based on constructed circulation analogues (see text
528 for details). Contours in (a) show observed sea-level pressure (SLP) trends (contour interval of
529 0.25 hPa per decade, negative values dashed); contours in (b) show the observed SLP trends
530 estimated from the constructed circulation analogues; contours in (c) based on the difference
531 between (a) and (b) are near-zero and not shown. Panel (d) shows the ensemble-mean temperature
532 and SLP trends from the 100-member CESM2 Large Ensemble (note that only the zero contour
533 shows up in panel d).
534

535 Precipitation is an inherently noisier field than temperature in both time and space, making it
536 challenging to extract the forced signal via "dynamical adjustment"; indeed, only one previous
537 study has attempted dynamical adjustment of observed precipitation trends (Guo et al. 2019).
538 Keeping in mind that the estimate of the circulation-induced component of precipitation trends
539 may be less robust than for temperature, we present the results as a proof-of-concept. Observed
540 precipitation trends during 1962-2021 are mainly driven by changes in atmospheric circulation,
541 with a small thermodynamic residual component (Fig. 13). This residual component bears some

https://doi.org/10.5194/npg-2022-15
Preprint. Discussion started: 19 October 2022

Nonlinear Processes in Geophysics
Discussions
Open Access
EGU

542 resemblance to the forced response in CESM2, particularly in terms of amplitude (~ 0.05 mm d-1
543 per decade; Fig. 13d). Notable areas of agreement in the sign of the trends include drying over
544 much of southern Europe and wetting over parts of northern Europe; central Europe shows less
545 agreement in polarity, unsurprisingly since this region was found to have lower signal-to-noise
546 than other areas.

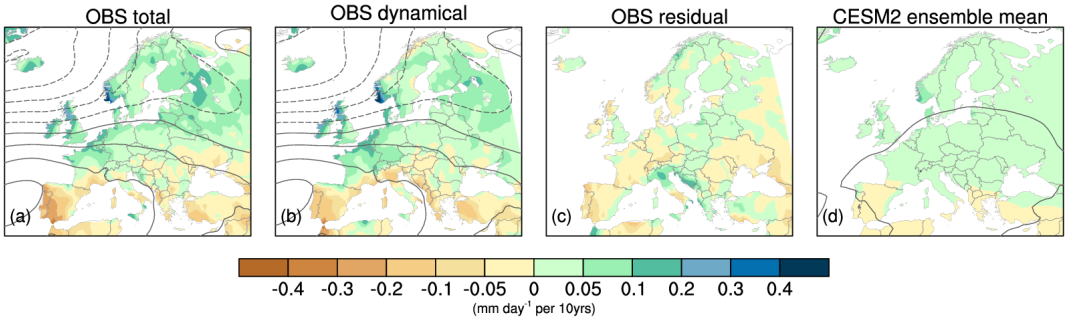

547

548 **Figure 13**. As in Fig. 12 but for precipitation (mm d^{-1} per decade).
549

550 ***g. Toward an observationally-based "range of outcomes"***

551 We conclude by bringing together the results of the Observational LE and "dynamical adjustment"
552 to produce a fully observationally-based estimate of the range of past 60-year trends in temperature
553 and precipitation. To the best of our knowledge, this is first time that these two approaches have
554 been combined. Specifically, we add the internal component of trends from each member of the
555 OBS LE to the thermodynamic-residual trend (the estimated observed forced response) obtained
556 from dynamical adjustment. As before, we select two contrasting ensemble members from the tails
557 of the distribution based on European-wide averages to illustrate the range of trend outcomes. The
558 "warm" end-member shows pronounced temperature increases over the northern two-thirds of the
559 continent, with maximum values in excess of 0.9 °C per decade, while the "cool" end-member
560 warms less than 0.2 °C per decade in most areas and even cools slightly over Ukraine and

https://doi.org/10.5194/npg-2022-15
Preprint. Discussion started: 19 October 2022

neighboring countries (Figs. 14 b and d, respectively). These divergent temperature trends are associated with contrasting SLP trends, with a positive NAO-like pattern in the "warm" member a negative (and eastward-shifted) NAO pattern in the "cool" member (Figs. 14 b and d). Qualitatively, this range of trend outcomes for both temperature and SLP is remarkably similar to that obtained directly from the CESM2 LE, with some regional differences in the location of cooling in the "cool" end-member (Figs. 14 e and g). There is no guarantee that the patterns and amplitudes of trends sampled in our selected end-members will agree between the model and observationally-based results, since there are many configurations that produce extremes in European-wide averages (not shown). That there is a strong qualitative resemblance between them is a testament to both the realism of the model's forced response and internal variability, and the efficacy of the OBS LE and dynamical adjustment approaches.

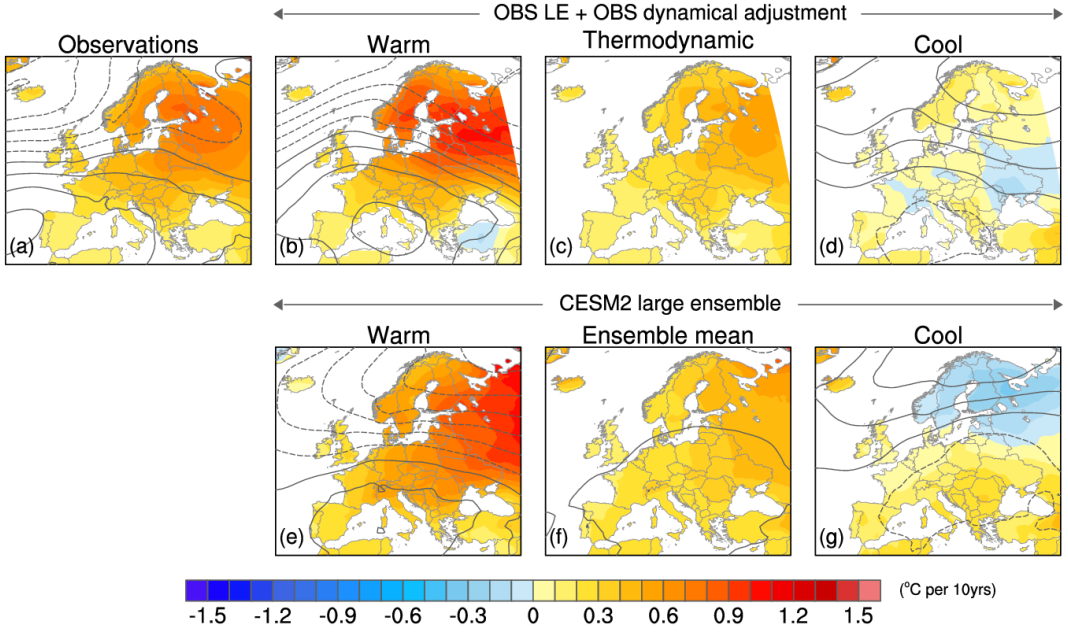

Figure 14. As in Fig. 10 but for the period 1962-2021. The top row is based on the Observational Large Ensemble combined with the residual thermodynamic component of observed trends. The bottom row is based on the 100-member CESM2 Large Ensemble. See text for details.

https://doi.org/10.5194/npg-2022-15
Preprint. Discussion started: 19 October 2022

576 Precipitation trends in the "wet" and "dry" end-members are also similar between the model and
577 observationally-based results (Fig. 15). The "wet" members show widespread increases in
578 precipitation over southern and central Europe (maximum values of 0.2-0.4 mm d^{-1} per decade)
579 and drying over the northern UK and parts of Scandinavia (Figs. 15 b and e). Largely opposite
580 patterns prevail in the "dry" members (Figs. 15 d and g). The contrasting precipitation trends in
581 the "wet" and "dry" end-members are associated with opposite flow configurations, with regions
582 of drying corresponding to high pressure and vice versa.

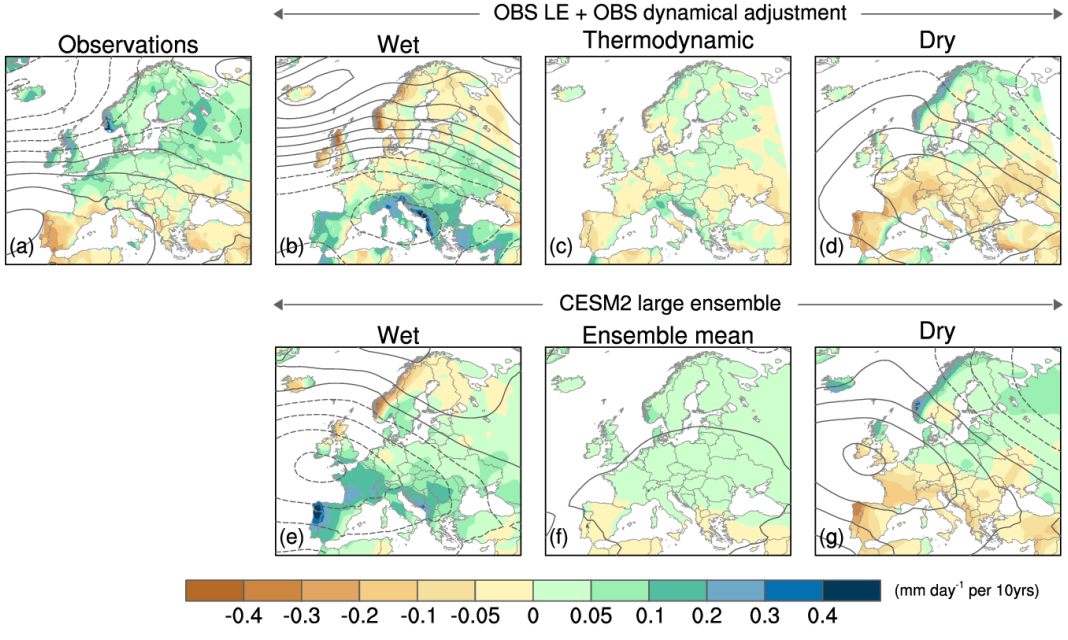

583

584 **Figure 15**. As in Fig. 14 but for precipitation (mm d^{-1} per decade).
585

586 **4. Summary and open questions**

587 Disentangling the effects of internal variability and anthropogenic forcing on regional climate
588 change remains a long-standing issue in climate sciences. Recent advances in climate modeling
589 and physical understanding have led to new insights on this topic, and provided an improved source

https://doi.org/10.5194/npg-2022-15
Preprint. Discussion started: 19 October 2022

590 of information on the future risks of climate and weather extremes associated with human-induced
591 climate change. Here, we have highlighted new findings for European winter climate based on the
592 following complementary tools: Earth System Model Large Ensemble simulations; an
593 observationally-based Large Ensemble; and an empirical approach for removing the influence of
594 internal atmospheric circulation variability from observed climate anomalies.
595
596 The new 100-member CESM2 Large Ensemble shows that internal climate variability imparts
597 considerably uncertainty to past and future 50-year trends in winter temperature and precipitation
598 over Europe. Such uncertainty is irreducible due to the lack of predictability of the simulated
599 internal variability on decadal time scales. A novel synthetic Large Ensemble constructed from the
600 statistical characteristics of internal variability in the observational record exhibits quantitatively
601 similar levels of uncertainty in past 50-year trends as the CESM2 LE, reinforcing the credibility
602 of the model's internally-generated trends. Additionally, the results of our "dynamical adjustment"
603 procedure applied to observations shows good agreement between the observed thermodynamic-
604 residual trend component and the model's forced thermodynamic trend, further underscoring the
605 realism of CESM2. Finally, for the first time, we have combined internal variability of trends from
606 an Observational Large Ensemble with an observational estimate of the forced trend (the
607 thermodynamic-residual component obtained from "dynamical adjustment") to show what the
608 observed range of past trends in European temperature and precipitation could have been. Because
609 it does not rely on climate model information, this observationally-based range of trend outcomes
610 provides a powerful test of the range of simulated trends in a model Large Ensemble.
611

https://doi.org/10.5194/npg-2022-15
Preprint. Discussion started: 19 October 2022

612 Many outstanding questions remain regarding the relative influences of internal climate variability
613 and anthropogenic forcing on regional climate change in models and the real world. Fortunately,
614 promising new tools are being developed to help address these challenges. For example, innovative
615 machine learning methods may be able to improve upon existing techniques for constructing
616 Observational Large Ensembles. Such methods have shown good results as statistical emulators
617 of model-based LEs, but their application to the observational record remains to be pursued
618 (Beusch et al. 2019). Similarly, neural network approaches to dynamical adjustment may offer
619 increased skill compared to conventional methods (Davenport and Diffenbaugh, 2021), but have
620 yet to be applied with the aim of separating forced and internal components of observed trends.
621 Complementary physically-based approaches such as Linear Inverse Modeling and Low-
622 Frequency Pattern Analysis mentioned in Section 1d also offer promise for estimating the forced
623 response in observations without reliance on climate models and should be pursued more widely.
624
625 We have relied on the fact that the CESM2 LE (like other models of its class; see Deser et al. 2020
626 and references therein) simulates a negligible forced atmospheric circulation trend over the past
627 50-60 years to interpret our observed dynamical adjustment results (i.e, we have equated the
628 observed dynamically-induced trend with the internal component, and the observed
629 thermodynamic-residual trend with the forced component). If the model is erroneous in this regard,
630 then our interpretation of our decomposition of observed trends into "internal dynamical" and
631 "forced thermodynamic" components is flawed. Indeed, recent work suggests that climate models
632 may be less predictable on seasonal-to-decadal timescales than the real world, particularly in terms
633 of the large-scale extra-tropical atmospheric circulation (the so-called "signal-to-noise" paradox;
634 e.g., Scaife et al. 2014; Eade et al. 2014; Scaife and Smith, 2018). But whether the results from

https://doi.org/10.5194/npg-2022-15
Preprint. Discussion started: 19 October 2022

such initial-value predictability studies carry over to models' forced atmospheric circulation responses to anthropogenic emissions remains an open question. Finally, a recent study by Strommen et al. (2002) finds that inclusion of stochastic parameterizations amplifies the simulated atmospheric circulation response to sea surface temperature and Arctic sea ice anomalies. Such stochastic parameterizations may represent unresolved air-sea coupling processes in "coarse-resolution" climate models such as CESM2. Emerging efforts to develop mesoscale-eddy-resolving global coupled climate models may provide more definitive answers to this elusive challenge in the near future.

Data and code availability statement

All data used in this study are publicly available as follows:

CESM2 Large Ensemble: https://www.earthsystemgrid.org/dataset/ucar.cgd.cesm2le.output.html

GPCC precipitation: https://www.dwd.de/EN/ourservices/gpcc/gpcc.html

BEST temperature: http://berkeleyearth.org/data/

and ERA5 SLP: https://www.ecmwf.int/en/forecasts/dataset/ecmwf-reanalysis-v5

Code used to create the Observational Large Ensemble and Dynamical Adjustment results are publicly available at:

https://github.com/karenamckinnon/observational_large_ensemble/ and

https://github.com/terrayl/Dynamico, respectively.

Author contributions

CD led the overall effort and wrote the manuscript. ASP performed some of the calculations and prepared the figures.

https://doi.org/10.5194/npg-2022-15
Preprint. Discussion started: 19 October 2022


Nonlinear Processes in Geophysics
Discussions
Open Access
EGU

658 **Competing interests**

659 The contact author has declared that none of the authors has any competing interests.

660

661 **Acknowledgements**

662 We acknowledge the efforts of all those who contributed to producing the model simulations and
663 observational data sets used in this study. We thank L. Terray for providing the dynamical
664 adjustment results and K. McKinnon for providing the observational large ensemble results. The
665 National Center for Atmospheric Research is sponsored by the National Science Foundation.

666

https://doi.org/10.5194/npg-2022-15
Preprint. Discussion started: 19 October 2022


Nonlinear Processes in Geophysics
Discussions
Open Access
EGU

667 **References**

668 Andrews, T., Bodas-Salcedo, A., Gregory, J. M., Dong, Y., Armour, K. C., Paynter, D., Lin, P.,
669 Modak, A., Mauritsen, T., Cole, J. N. S., Medeiros, B., Benedict, J. J., Douville, H.,
670 Roehrig, R., Koshiro, T., Kawai, H., Ogura, T., Dufresne, J. -L., Allan, R. P., and Liu, C.:
671 On the effect of historical SST patterns on radiative feedback, J. Geophys. Res.-Atmos.,
672 127, e2022JD036675, https://doi.org/10.1029/2022JD036675, 2022.
673 Barnes, E. A., Hurrell, J. W., and Uphoff, I. E.: Viewing forced climate patterns through an AI
674 lens, Geophys. Res. Lett., 46, 13389–13398, https://doi.org/10.1029/2019GL084944, 2019.
675 Beusch, L., Gudmundsson, L., and Seneviratne, S. I.: Emulating Earth System Model
676 temperatures: from global mean temperature trajectories to grid-point level realizations on
677 land, Earth Syst. Dyn. Discuss., https://doi.org/10.5194/esd-2019-34, 2019.
678 Bonfils, C. J. W., Santer, B. D., Fyfe, J. C., Marvel, K., Phillips, T. J., and Zimmerman, S. R. H.:
679 Human influence on joint changes in temperature, rainfall and continental aridity. Nat.
680 Clim. Change, 10, 726-731, https://doi.org/10.1038/s41558-020-0821-1, 2020.
681 Branstator, G. and Teng, H.: Two limits of initial-value decadal predictability in a CGCM, J.
682 Climate, 23, 6292-6311, https://doi.org/10.1175/2010JCLI3678.1, 2010.
683 Capotondi, A., Deser, C., Phillips, A., Okumura, Y. and Larson, S.: ENSO and Pacific
684 DecadalVvariability in the Community Earth System Model Version 2, J. Adv. Model.
685 Earth Sy., 12, e2019MS002022, https://doi.org/10.1029/2019MS002022, 2020.
686 Compo, G. P., Whitaker, J. S., Sardeshmukh, P. D., Matsui, N., Allan, R. J., Yin, X., Gleason,
687 B.E., Vose, R.S., Rutledge, G., Bessemoulin, P., Brönnimann, S., Brunet, M., Crouthamel,
688 R.I., Grant, A.N., Groisman, P.Y., Jones, P.D., Kruk, M.C., Kruger, A.C., Marshall, G.J.,
689 Maugeri, M., Mok, H.Y., Nordli, Ø., Ross, T.F., Trigo, R.M., Wang, X.L., Woodruff, S.D.

https://doi.org/10.5194/npg-2022-15
Preprint. Discussion started: 19 October 2022

690 and Worley, S.J.: The twentieth century reanalysis project, Q. J. Roy. Meteor. Soc., 137, 1–
691 28, https://doi.org/10.1002/qj.776, 2011.
692 Davenport, F. V. and Diffenbaugh, N. S.: Using machine learning to analyze physical causes of
693 climate change: A case study of U.S. Midwest extreme precipitation, Geophys. Res.
694 Lett., 48, e2021GL093787. https://doi.org/10.1029/2021GL093787, 2021.
695 Deser, C., Phillips, A., Bourdette, V., and Teng, H. Y.: Uncertainty in climate change
696 projections: The role of internal variability, Clim. Dynam., 38, 527–546.
697 https://doi.org/10.1007/s00382-010-0977-x, 2012.
698 Deser, C., Phillips, A., Alexander, M. A., and Smoliak, B. V.: Projecting North American
699 climate over the next 50 years: Uncertainty due to internal variability. J. Climate, 27, 2271–
700 2296, https://doi.org/10.1175/JCLI-D-13-00451.1, 2014.
701 Deser, C., Terray, L., and Phillips, A. S.: Forced and internal components of winter air
702 temperature trends over North America during the past 50 years: Mechanisms and
703 implications, J. Climate, 29, 2237–2258. https://doi.org/10.1175/JCLI-D-15-0304.1, 2016.
704 Deser, C., Simpson, I. R., McKinnon K. A., and Phillips, A. S.: The Northern Hemisphere extra-
705 tropical atmospheric circulation response to ENSO: How well do we know it and how do
706 we evaluate models accordingly? J. Climate, 30, 5059-5082, https://doi.org/10.1175/JCLI-
707 D-16-0844.1, 2017.
708 Deser, C., Hurrell, J. W., and Phillips, A.S.: The role of the North Atlantic Oscillation in
709 European Climate Projections, Clim. Dynam., 49, 3141–3157,
710 https://doi.org/10.1007/s00382-016-3502-z, 2017.

https://doi.org/10.5194/npg-2022-15
Preprint. Discussion started: 19 October 2022


Nonlinear Processes in Geophysics Discussions
Open Access
EGU

711 Deser, C., Simpson, I. R., Phillips, A. S., and McKinnon, K.A.: How well do we know ENSO's
712 climate impacts over North America, and how do we evaluate models accordingly? J.
713 Climate, 30, 4991-5014, https://doi.org/10.1175/JCLI-D-17-0783.1, 2018.
714 Deser, C.: Certain uncertainty: The role of internal climate variability in projections of regional
715 climate change and risk management. Earths Future, 8, e2020EF001854,
716 https://doi.org/10.1029/2020EF001854, 2020.
717 Deser, C., Lehner, F., Rodgers, K. B., Ault, T., Delworth, T. L., DiNezio, P. N., Fiore, A.,
718 Frankignoul, C., Fyfe, J. C., Horton, D. E., Kay, J. E., Knutti, R., Lovenduski, N. S.,
719 Marotzke, J., McKinnon, K. A., Minobe, S., Randerson, J., Screen, J. A, Simpson, I. R.,
720 and Ting, M.: Insights from earth system model initial-condition large ensembles and
721 future prospects. Nat. Clim. Change, 10, 277-286, https://doi.org/10.1038/s41558-020-
722 0731-2, 2020.
723 Deser, C., Phillips, A. S., Simpson, I. R., Rosenbloom, N., Coleman, D., Lehner, F., Pendergrass,
724 A., DiNezio, P., and Stevenson, S.: Isolating the Evolving Contributions of Anthropogenic
725 Aerosols and Greenhouse Gases: A New CESM1 Large Ensemble Community Resource. J.
726 Climate, 33, 7835-7858, https://doi.org/10.1175/JCLI-D-20-0123.1, 2020.
727 Deser, C. and Phillips, A.S.: Defining the internal component of Atlantic Multidecadal
728 Variability in a changing climate. Geophys. Res. Lett., 48, e2021GL095023,
729 https://doi.org/10.1029/2021GL095023, 2021.
730 DiNezio, P. N., Deser, C., Okumura, Y., and Karspeck, A.: Predictability of 2-year La Niña
731 events in a coupled general circulation model, Clim. Dyn. 49, 4237–4261, 2017.

https://doi.org/10.5194/npg-2022-15
Preprint. Discussion started: 19 October 2022

732 Dong, Y, Armour, K.C., Zelinka, M., Proistosescu, C., Battisti, D., Zhou, C., and Andrews, T.:
733 Inter-model spread in the pattern effect and its contribution to climate sensitivity in CMIP5
734 and CMIP6 models, J. Climate, https://doi.org/10.1175/JCLI-D-19-1011.1, 2020.
735 Eade, R., Smith, D., Scaife, A., Wallace, E., Dunstone, N., Hermanson, L., and Robinson, N.: Do
736 seasonal-to-decadal climate predictions underestimate the predictability of the real
737 world?, Geophys. Res. Lett., 41, 5620– 5628, https://doi.org/10.1002/2014GL061146,
738 2014.
739 Fasullo, J., Phillips, A. S., and Deser, C.: Evaluation of leading modes of climate variability in
740 the CMIP Archives, J. Climate, 33, 5527–5545, https://doi.org/10.1175/JCLI-D-19-1024.1,
741 2020.
742 Gordon, E. M. and Barnes, E.A.: Incorporating uncertainty into a regression neural network
743 enables identification of decadal state-dependent predictability, Geophys. Res. Lett.,
744 e2022GL098635, https://doi.org/10.1029/2022GL098635, 2022.
745 Gould, S. J.: Wonderful Life: The burgess shale and the nature of history, W. W. Norton & Co.,
746 978-0-393-30700-9, 1989.
747 Griffies, S. M. and Bryan, K.: Predictability of North Atlantic multidecadal climate
748 variability, Science, 275, 181–184, https://doi.org/10.1126/science.275.5297.181, 1997.
749 Guo, R. X., Deser, C., Terray, L., and Lehner, F.: Human influence on terrestrial precipitation
750 trends revealed by dynamical adjustment, Geophys. Res. Lett., 46, 3426-3434,
751 https://doi.org/10.1029/2018GL081316, 2019.
752 Hegerl, G.C., Zwiers, F. W. , Braconnot, P., Gillett, N. P., Luo, Y., Marengo Orsini, J. A.,
753 Nicholls, N., Penner, J. E., and Stott, P. A.: Understanding and attributing climate change.
754 In: Climate Change 2007: The Physical Science Basis. Contribution of Working Group I to

https://doi.org/10.5194/npg-2022-15
Preprint. Discussion started: 19 October 2022

the Fourth Assessment Report of the Intergovernmental Panel on Climate Change, Solomon, S., D. Qin, M. Manning, Z. Chen, M. Marquis, K.B. Averyt, M. Tignor and H.L. Miller (eds.), Cambridge University Press, Cambridge, United Kingdom and New York, NY, USA, 2007.

Hurrell J. W., Kushnir, Y., Ottersen G., and Visbeck M. (eds): The North Atlantic Oscillation: climate significance and environmental impact, Geophys. Monogr. Ser, 134, AGU, Washington, D. C, 2003.

James, I. N. and James, P. M.: Spatial structure of ultra-low-frequency variability of the flow in a simple atmospheric circulation model. Quart. J. Roy. Meteor. Soc., 118, 1211-1233, https://doi.org/10.1002/qj.49711850810, 1992.

Jin, E.K., Kinter, J.L., and Wang, B: Current status of ENSO prediction skill in coupled ocean–atmosphere models, Clim. Dynam. 31, 647–664, https://doi.org/10.1007/s00382-008-0397-3, 2008.

Kay, J., Deser, C., Phillips, A., Mai, A., Hannay, C., Strand, G., Arblaster, J. M., Bates, S. C., Danabasoglu, G., Edwards, J., Holland, M., Kushner, P., Lamarque, J. -F., Lawrence, D., Lindsay, K., Middleton, A., Munoz, E., Neale, R., Oleson, K., Polvani, L. and Vertenstein, M.: The Community Earth System Model (CESM) Large Ensemble Project: A community resource for studying climate change in the presence of internal climate variability, B. Am. Meteorol. Soc., 96, 1333–1349, https://doi.org/10.1175/BAMS-D-13-00255.1, 2015.

Klavans, J.M., Cane, M.A., Clement, A.C., and Murphy, L. N.: NAO predictability from external forcing in the late 20th century, Npj Clim. Atmos. Sci., 4, 22 (2021), https://doi.org/10.1038/s41612-021-00177-8, 2021.

https://doi.org/10.5194/npg-2022-15
Preprint. Discussion started: 19 October 2022

777 Lehner, F., Schurer, A. P., Hegerl, G. C., Deser, C., and Frölicher, T. L.: The importance of
778 ENSO phase during volcanic eruptions for detection and attribution, Geophys. Res. Lett.
779 43, 2851–2858, https://doi.org/10.1002/2016GL067935, 2016.
780 Lehner, F., Deser, C., and Terray, L.: Towards a new estimate of "time of emergence" of
781 anthropogenic warming: insights from dynamical adjustment and a large initial-condition
782 model ensemble. J. Climate, 30, 7739-7756, http://doi.org/10.1175/JCLI-D-16-0792.1,
783 2017.
784 Lehner, F., Deser, C., Simpson, I. R., and Terray, L.: Attributing the US Southwest's recent shift
785 into drier conditions, Geophys. Res. Lett., 45, 6251–6261,
786 https://doi.org/10.1029/2018GL078312, 2018.
787 Lehner, F., Deser, C., Maher, N., Marotzke, J., Fischer, E., Brunner, L., Knutti, R. and Hawkins,
788 E.: Partitioning climate projection uncertainty with multiple large ensembles and
789 CMIP5/6. Earth Syst. Dynam. Discuss., Special Issue on Large Ensembles, 11, 491–508,
790 https://doi.org/10.5194/esd-11-491-2020, 2020.
791 Leith, C. E.: The standard error of time-average estimates of climatic means, J. Appl. Meteorol.
792 Clim., 12(6), 1066-1069, https://doi.org/10.1175/1520-
793 0450(1973)012%3C1066:TSEOTA%3E2.0.CO;2, 1973.
794 Lorenz, E. N.: Deterministic nonperiodic flow, J. Atmos. Sci., 20, 130–141,
795 https://doi.org/10.1175/1520-0469(1963)020<0130:DNF>2.0.CO;2, 1963.
796 Madden, R. A.: Estimates of the natural variability of time-averaged sea-level pressure, Mon.
797 Weather. Rev., 104, 942-952, https://doi.org/10.1175/1520-
798 0493(1976)104%3C0942:EOTNVO%3E2.0.CO;2, 1975.

https://doi.org/10.5194/npg-2022-15
Preprint. Discussion started: 19 October 2022

799 Maher, N., Matei, D., Milinski, S., and Marotzke, J.: ENSO change in climate projections:
800 Forced response or internal variability?, Geophys. Res. Lett., 45, 11390–11398,
801 https://doi.org/10.1029/2018GL079764, 2018.
802 Maher, N., Milinski, S., Suarez-Gutierrez, L., Botzet, M., Dobrynin, M., Kornblueh, L., Kröger,
803 J., Takano, Y., Ghosh, R., Hedemann, C., Li, C., Li, H., Manzini, E., Notz, D. Putrasahan,
804 D., Boysen, L., Claussen, M., Ilyina, T., Olonscheck, D., Raddatz, T., Stevens, B., and
805 Marotzke, J.: The Max Planck Institute Grand Ensemble: Enabling the exploration of
806 climate system variability, J. Adv. Model. Earth Sy., 11, 2050–2069,
807 https://doi.org/10.1029/2019MS001639, 2019.
808 McGraw, M. C., Barnes, E. A., and Deser, C.: Reconciling the observed and modeled southern
809 hemisphere circulation response to volcanic eruptions, Geophys. Res. Lett., 43, 7259–7266,
810 https://doi.org/10.1002/2016GL069835, 2016.
811 McKenna, C. M., and Maycock, A. C.: Sources of uncertainty in multimodel large ensemble
812 projections of the winter North Atlantic Oscillation, Geophys. Res. Lett., 48,
813 e2021GL093258, https://doi.org/10.1029/2021GL093258, 2021.
814 McKinnon, K. A and Deser, C.: Internal variability and regional climate trends in an
815 Observational Large Ensemble, J. Climate, 31, 6783–6802, https://doi.org/10.1175/JCLI-
816 D-17-0901.1, 2018.
817 McKinnon, K. A. and Deser, C.: The inherent uncertainty of precipitation variability, trends, and
818 extremes due to internal variability, with implications for Western US water resources, J.
819 Climate, 34, 9605-9622, https://doi.org/10.1175/JCLI-D-21-0251.1, 2021.

https://doi.org/10.5194/npg-2022-15
Preprint. Discussion started: 19 October 2022

820 Meehl, G., Hu, A. and Teng, H: Initialized decadal prediction for transition to positive phase of
821 the Interdecadal Pacific Oscillation, Nat. Commun., 7, 11718 (2016),
822 https://doi.org/10.1038/ncomms11718, 2016.
823 Meehl, G.A., J.H. Richter, Teng, H., Capotondi, A., Cobb, K., Doblas-Reyes, F., Donat, M. G.,
824 England, M. H., Fyfe, J. C., Han, W., Kim, H., Kirtman, B. P., Kushnir, Y., Lovenduski, N.
825 S., Mann, M. E., Merryfield, W. J., Nieves, V., Pegion, K., Rosenbloom, N., Sanchez, S.
826 C., Scaife, A. A., Smith, D., Subramanian, A. C., Sun, L., Thompson, D., Ummenhofer, C.
827 C., and Xie, S. -P.: Initialized Earth system prediction from subseasonal to decadal
828 timescales, Nat. Rev. Earth Environ., 2, 340–357 (2021), https://doi.org/10.1038/s43017-
829 021-00155-x, 2021.
830 Merrifield, A., Lehner, F., Xie, S. -P., and Deser, C.: Removing circulation effects to assess
831 Central US land-atmosphere interactions in the CESM Large Ensemble, Geophys. Res.
832 Lett., 44, 9938-9946, https://doi.org/10.1002/2017GL074831, 2017.
833 Milinski, S., Maher, N., and Olonscheck, D.: How large does a large ensemble need to be?, Earth
834 Syst. Dyn. Discuss., 11, 885-901, https://doi.org/10.5194/esd-11-885-2020, 2019.
835 Newman, M.: Interannual to decadal predictability of tropical and North Pacific sea surface
836 temperatures, J. Climate, 20, 2333–2356, https://doi.org/10.1175/JCLI4165.1, 2007.
837 Newman, M., Alexander, M. A., Ault, T. R., Cobb, K. M., Deser, C., Di Lorenzo, E., Mantua, N.
838 J., Miller, A. J., Minobe, S., Nakamura, H., Schneider, N., Vimont, D. J., Phillips, A. S.,
839 Scott, J. D., and Smith, C. A.: The Pacific decadal oscillation, revisited, J. Climate, 29,
840 4399–4427, https://doi.org/10.1175/ JCLI-D-15-0508.1, 2016.

https://doi.org/10.5194/npg-2022-15
Preprint. Discussion started: 19 October 2022

841 O'Brien, J. P. and Deser, C.: Quantifying and understanding forced changes to unforced modes
842 of atmospheric circulation variability over the North Pacific in a coupled model large
843 ensemble, J. Climate, https://doi.org/10.1175/JCLI-D-22-0101.1, 2022.
844 Olivarez, H. C., Lovenduski, N. S., Brady, R. X., Fay, A. R., Gehlen, M., Gregor, L.,
845 Landschützer, P., McKinley, G. A., McKinnon, K. A., and Munro, D. R.: Alternate
846 histories: Synthetic large ensembles of sea-air CO_2 flux, Global Biogeochem. Cy., 36,
847 e2021GB007174, https://doi.org/10.1029/2021GB007174, 2022.
848 Persad, G. G., and Caldeira, K.: Divergent global-scale temperature effects from identical
849 aerosols emitted in different regions. Nat. Commun., 9, 3289,
850 https://doi.org/10.1038/s41467- 018-05838-6, 2018.
851 Rodgers, K. B., Lee, S. -S., Rosenbloom, N., Timmermann, A., Danabasoglu, G., Deser, C.,
852 Edwards, J., Kim, J. -E., Simpson, I., Stein, K., Stuecker, M. F., Yamaguchi, R., Bodai, T.,
853 Chung, E. -S., Huang, L., Kim, W., Lamarque, J. -F., Lombardozzi, D., Wieder, W. R., and
854 Yeager, S. G.: Ubiquity of human-induced changes in climate variability. Earth Sys.
855 Dyn., 12, 1393–1411, https://doi.org/10.5194/esd-12-1393-2021, 2021.
856 Rohde, R., Muller, R., Jacobsen, R., Perlmutter, S., Rosenfeld, A., Wurtele, J., Curry, J.,
857 Wickham, C., and Mosher, S.: Berkeley Earth temperature averaging process, Geoinf.
858 Geostat. Overview, 1:2, https://doi.org/10.4172/2327-4581.1000103, 2013.
859 Santer, B., Fyfe, J. C., Solomon, S., Painter, J. F., Bonfils, C., Pallotta, G., and Zelinka, M. D.:
860 Quantifying stochastic uncertainty in detection time of human-caused climate signals, Proc.
861 Natl. Acad. Sci., 116, 19821–19827, https://doi.org/10.1073/pnas.1904586116, 2019.
862 Scaife, A. A., Arribas, A., Blockley, E., Brookshaw, A., Clark, R. T., Dunstone, N., Eade, R.,
863 Fereday, D., Folland, C. K., Gordon, M., Hermanson, L., Knight, J. R., Lea, D. J.,

https://doi.org/10.5194/npg-2022-15
Preprint. Discussion started: 19 October 2022

MacLachlan, C., Maidens, A., Martin, M., Peterson, A. K., Smith, D., Vellinga, M., Wallace, E., Waters, J. and Williams, A: Skillful long-range prediction of European and North American winters, Geophys. Res. Lett., 41, 2514–2519, https://doi.org/10.1002/2014GL059637, 2014.

Scaife, A. A. and Smith, D.: A signal-to-noise paradox in climate science. Npj Clim. Atmos. Sci., 1, 28 (2018), https://doi.org/10.1038/s41612-018-0038-4, 2018.

Schneider, D. P., Deser, C., and Fan, T.: Comparing the impacts of tropical SST variability and polar stratospheric ozone loss on the Southern Ocean westerly winds, J. Climate, 28, 9350-9372, https://doi.org/10.1175/JCLI-D-15-0090.1, 2015.

Schneider, U., Fuchs, T., Meyer-Christoffer, A., and Rudolf, B.: Global precipitation analysis products of the GPCC. Global Precipitation Climatology Centre (GPCC), DWD, Internet Publikation, 1-12.

Shepherd, T.: Atmospheric circulation as a source of uncertainty in climate change projections, Nature Geosci., 7, 703–708 (2014), https://doi.org/10.1038/ngeo2253, 2014.

Sippel, S. Meinshausen, N., Merrifield, A., Lehner, F., Pendergrass, A. G., Fischer, E., and Knutti, R.: Uncovering the forced climate response from a single ensemble member using statistical learning, J. Climate, 32, 5677-5699, https://doi.org/10.1175/JCLI-D-18-0882.1, 2019.

Smith, D., Eade, R., Scaife, A. A., Caron, L. -P., Danabasoglu, G., DelSole, T. M., Delworth, T., Doblas-Reyes, F. J., Dunstone, N. J., Hermanson, L., Kharin, V., Kimoto, M., Merryfield, W. J., Mochizuki, T., Müller, W. A., Pohlmann, H., Yeager, S., and Yang, X: Robust skill of decadal climate predictions, Npj Clim. Atmos. Sci., 2, 13 (2019), https://doi.org/10.1038/s41612-019-0071-y, 2019.

https://doi.org/10.5194/npg-2022-15
Preprint. Discussion started: 19 October 2022

887 Smith, D. M. et al. North Atlantic Climate far more predictable than models imply, Nature, 583,
888 796–800 (2020), 2020.
889 Smith, D. M., Scaife, A. A., Eade, R., Athanasiadis, P., Bellucci, A., Bethke, I., Bilbao, R.,
890 Borchert, L. F., Caron, L.P., Counillon, F., Danabasoglu, G., Delworth, T., Doblas-Reyes,
891 F. J., Dunstone, N.J., Estella-Perez, V., Flavoni, S., Hermanson, L., Keenlyside, N., Kharin,
892 V., Kimoto, M., Merryfield, W. J., Mignot, J., Mochizuki, T., Modali, K., Monerie, P. A.,
893 Müller, W. A., Nicolí, D., Ortega, P., Pankatz, K., Pohlmann, H., Robson, J., Ruggieri, P.,
894 Sospedra-Alfonso, R., Swingedouw, D., Wang, Y., Wild, S., Yeager, S., Yang, X., and
895 Zhang, L.: North Atlantic climate far more predictable than models imply, Nature, 583,
896 796-800, https://doi.org/10.1038/s41586-020-2525-0, 2020.
897 Smoliak, B. V., Wallace, J. M., Lin, P., and Fu, Q.: Dynamical adjustment of the Northern
898 Hemisphere surface air temperature field: Methodology and application to observations, J.
899 Climate, 28, 1613–1629. https://doi.org/10.1175/JCLI-D-14-00111.1, 2015.
900 Stevenson, S., Fox-Kemper, B., Jochum, M., Neale, R., Deser, C., and Meehl, G.: Will there be
901 a significant change to El Nino in the 21st Century?, J. Climate, 25, 2129-2145,
902 https://doi.org/10.1175/JCLI-D-11-00252.1, 2012.
903 Strommen, K., Juricke, S., and Cooper, F.: Improved teleconnection between Arctic sea ice and
904 the North Atlantic Oscillation through stochastic process representation, Weather Clim.
905 Dynam., 3, 951–975, https://doi.org/10.5194/wcd-3-951-2022, 2022.
906 Suarez-Gutierrez, L., Milinski, S., and Maher, N.: Exploiting large ensembles for a better yet
907 simpler climate model evaluation, Clim. Dynam., 57, 2557–2580 (2021),
908 https://doi.org/10.1007/s00382-021-05821-w, 2021.

https://doi.org/10.5194/npg-2022-15
Preprint. Discussion started: 19 October 2022

909 Swart, N. C., Fyfe, J. C., Hawkins, E., Kay, J. E., and Jahn A.: Influence of internal variability on
910 Arctic sea-ice trends. Nat. Clim. Change, 5, 86–89, https://doi.org/10.1038/nclimate2483,
911 2015.
912 Tebaldi, C., Dorheim, K., Wehner, M., Leung, R.: Extreme metrics from large ensembles:
913 investigating the effects of ensemble size on their estimates, Earth Syst. Dynam., 12 (4),
914 1427-1501, https://doi.org/10.5194/esd-12-1427-2021, 2021.
915 Tél, T., Bódai, T., Drótos, G., Haszpra, T., Herein, M., Kaszás, B., and Vincze, M.: The theory
916 of parallel climate realizations, J. Stat, Phys., 179, 1496–1530,
917 https://doi.org/10.1007/s10955-019-02445-7, 2020.
918 Terray, L.: A dynamical adjustment perspective on extreme event attribution, Weather Clim.
919 Dynam., 2, 971–989, https://doi.org/10.5194/wcd-2-971-2021, 2021.
920 Thompson, D. W. J., Barnes, E. A., Deser, C., Foust, W. E., and Phillips, A. S.: Quantifying the
921 role of internal climate variability in future climate trends, J. Climate, 28, 6443–6456,
922 https://doi.org/10.1175/JCLI-D-14-00830.1, 2015.
923 Trenary, L. and DelSole, T.: Does the Atlantic Multidecadal Oscillation Get Its Predictability
924 from the Atlantic Meridional Overturning Circulation?, J. Climate, 29, 5267-5280,
925 https://doi.org/10.1175/JCLI-D-16-0030.1, 2016.
926 Wallace, J.M., Deser, C., Smoliak, B. V., and Phillips, A. S.: Attribution of climate change in
927 the presence of internal variability, In Climate Change: Multidecadal and Beyond (Eds:
928 C.P. Chang, M. Ghil, M. Latif, and J. M. Wallace), World Scientific Series on Asia-Pacific
929 Weather and Climate, 6, 1-29, https://doi.org/10.1142/9789814579933_0001, 2013.
930 Wang, C., Deser, C., Yu, J. -Y., DiNezio, P., and Clement, A.: El Nino and Southern Oscillation
931 (ENSO): A Review. Coral Reefs of the Eastern Pacific, P. Glymn, D. Manzello and I.

https://doi.org/10.5194/npg-2022-15
Preprint. Discussion started: 19 October 2022

Enochs, Eds., Springer Science Publisher, 4, 85-106, https://doi.org/10.1007/978-94-017-7499-4_4, 2017.

Wills, R. C. J., Battisti, D. S., Armour, K. C., Schneider, T., and Deser, C.: Pattern recognition methods to separate forced responses from internal variability in climate model ensembles and observations, J. Climate, 33, 8693-8719, https://doi.org/10.1175/JCLI-D-19-0855.1, 2020.

Wittenberg, A. T.: Are historical records sufficient to constrain ENSO simulations?, Geophys. Res. Lett., 36, L12702, https://doi.org/10.1029/2009GL038710, 2009.

Wu, X., Okumura, Y. M., Deser, C., and DiNezio, P. N.: Two-year dynamical predictions of ENSO event duration during 1954–2015, J. Climate, 34(10), 4069-4087, https://doi.org/10.1175/JCLI-D-20-0619.1, 2021.

Yeager, S. Danabasoglu, D., Rosenbloom, N. A., Strand, W., Bates, S. C., Meehl, G. A., Karspeck, A. R., Lindsay, K., Long, M. C., Teng, H., and Lovenduski, N. S.: Predicting near-term changes in the Earth System: A large ensemble of initialized decadal prediction simulations using the Community Earth System Model, Bull. Am. Meteorol. Soc. 99, 1867–1886, https://doi.org/10.1175/BAMS-D-17-0098.1, 2018.

Zhang, R., Sutton, R., Danabasoglu, G., Kwon, Y.-O., Marsh, R., Yeager, S. G., Amrhein, D. E., and Little, C. M.: A review of the role of the Atlantic Meridional Overturning Circulation in Atlantic Multidecadal Variability and associated climate impacts, Rev. Geophys., 57, 316–375, https://doi.org/10.1029/2019RG000644, 2019.